

Analysis of path integrals at low temperature: Box formula, occupation time and ergodic approximation

Sébastien Paulin, Angel Alastuey, Thierry Dauxois

Laboratoire de Physique, UMR-CNRS 5672, ENS Lyon, 46 Allée d'Italie, 69364 Lyon cédex 07, France

(Dated: September 21, 2018)

We study the low temperature behaviour of path integrals for a simple one-dimensional model. Starting from the Feynman-Kac formula, we derive a new functional representation of the density matrix at finite temperature, in terms of the occupation times of Brownian motions constrained to stay within boxes with finite sizes. From that representation, we infer a kind of ergodic approximation, which only involves double ordinary integrals. As shown by its applications to different confining potentials, the ergodic approximation turns out to be quite efficient, especially in the low-temperature regime where other usual approximations fail.

PACS numbers: 05.30.-d Quantum statistical mechanics; 05.40.Jc Brownian motion

I. INTRODUCTION

The knowledge of the density matrix at finite temperature T for few interacting particles, is of paramount importance for studying equilibrium properties of quantum many-body systems. Indeed, such density matrices occur in low-fugacity expansions, while they are also key ingredients in quantum Monte Carlo simulations. In this context, the Feynman-Kac (FK) representation of the density matrix in terms of path integrals [1, 2] is particularly useful. On the one hand, it has been used for deriving exact (analytical) expressions for simple models [3]. On the other hand, beyond the well-known Wigner-Kirkwood expansion [4, 5, 6] around the classical limit, various approximations, non-perturbative in \hbar , have been introduced within that framework: for instance, the celebrated semi-classical approximation [1] (widely used in numerous situations), the variational approach of Feynman and Kleinert [7], or the renormalized Wigner-Kirkwood scheme.

The FK representation is described in Sec. II. For the sake of simplicity, we consider the simple case of a single particle in one dimension submitted to a stationary confining potential. The mean spatial extension of the brownian paths, which intervene in the FK representation, is controlled by the thermal de Broglie wavelength of the quantum particle. At high temperatures, since that extension vanishes, exact asymptotic expansions, as well as direct numerical estimations, become rather straightforward. At the analytical level, Wigner-Kirkwood \hbar^2 -expansions around the classical limit, which have been derived long ago in other frameworks, are easily recovered. On the computational side, functional integration over paths can be replaced, within a good accuracy, by ordinary integrals over a discrete set of parameters, via the use of either free propagators in Trotter formula [8] or simple modelizations of brownian paths [9]. However, at low temperatures, similar calculations loose accuracy, while they also become rather time-consuming. Moreover, the corresponding asymptotic structure of the density matrix, provided by the groundstate contribution in its spectral expression, does not clearly emerge from its FK representation. In fact, in that temperature regime, the average extension of paths diverge, whereas the main contribution to the functional integral arises from paths with a finite extension, of the order of the localization length of the ground state: contributions of such minority paths are significantly different from the average contribution. Most of our knowledge is negative, i.e. tells us which trajectories are not important [10], so, in some sense, we will try to have a positive attitude [11].

In this paper, we derive a new functional representation of the density matrix, which is more suitable than the genuine FK formula for tackling the low-temperature regime (see Sec. III). The starting central observations are described in Sec. III.A. First, in the FK functional integral, only marginal paths with finite extensions (i.e. large deviations with respect to the average) contribute when T goes to zero. Second, many of such paths with quite different jagged shapes, provide similar contributions, mainly determined by the corresponding local occupation times. Thus, it is quite natural to collect paths into sets defined by their spatial extension and their local occupation times. That procedure allows us to transform exactly FK representation (10) into the so-called box formula (35). That formula is defined via the introduction of paths constrained to stay in a box with size ℓ and characterized by an intermediate flight time s (in $\beta\hbar$ units with $\beta = 1/k_B T$). It involves a double ordinary integral over ℓ and s , combined to functional integrals over local occupation times associated with the constrained paths. As required, box formula (35) provides a better understanding of the low-temperature behaviour of the density matrix than FK representation (10). When T vanishes, leading contributions obviously arise from typical sizes ℓ much smaller than de Broglie wavelength. In a forthcoming paper, we will argue how groundstate quantities emerge from box formula (35), by using scaling properties of the probability distribution function (PDF) of occupation times at low temperatures.

Beyond its conceptual interest for understanding low-temperature behaviours of path integrals, box formula (35) also allows us to derive new approximations. This is illustrated in Section IV, where we present the so-called ergodic approximation. That approximation results from the truncation to first order of cumulant expansions of the functional averages. It amounts to replace each local occupation time associated with a given constrained path, by its average over the PDF of such occupation times. This can be viewed as some kind of ergodic hypothesis, because the (imaginary) time average of the potential experienced by the particle along that path, is then replaced by a spatial average with a measure defined by the previous mean occupation-time. Ergodic expression (39) involves only an ordinary double integral over ℓ and s . The key ingredient, namely the mean occupation-time (in units of $1/\ell$), depends on three dimensionless parameters. Using its low and high temperature behaviours (derived analytically), we propose simple tractable expressions for that quantity, which turn out to be quite accurate at any temperature.

Section V is devoted to the applications of the ergodic approximation to various simple forms of the confining potential. First, we determine the asymptotic analytical forms of the approximate density matrices at both low and high temperatures. When T diverges, Wigner-Kirkwood expansion is partially recovered. When T vanishes, the main features of the exact behaviours are well reproduced. The approximate density matrices then do factorize as a product of a Boltzmann factor associated with a given energy, times a function of position only: this provides satisfactory approximate expressions for the groundstate energy and wavefunction. Second, numerical calculations are performed at finite intermediate temperatures. As expected from the previous analytical results, the ergodic approximation turns out to be quite reasonably accurate over the whole range of considered temperatures, and discrepancies with (numerically) exact results (in part inferred from the spectral representation) do not exceed a few percent. Moreover, it significantly improves over the well-known semi-classical approximation, which completely fails at low temperatures (except of course for the harmonic potential where semi-classical calculations become exact).

Further applications and extensions of our approach will be presented elsewhere. In particular, the ergodic approximation can be applied to unconfined potentials, and it can be straightforwardly extended to higher dimensions and to systems with several particles. Furthermore, other approximations might be easily introduced by starting from box formula as argued at the end of Section III.

II. PATH INTEGRAL FRAMEWORK

In this Section, we first define the model and then introduce the FK representation of the corresponding density matrix. Next, we briefly recall the efficiency of FK formula for describing the high-temperature regime, and we argue about its drawbacks for analyzing low-temperature behaviours.

A. The model

We consider a quantum non-relativistic particle of mass m in one dimension z , submitted to a confining potential V , i.e $V(z) \rightarrow \infty$ when $|z| \rightarrow \infty$. Its Hamiltonian reads

$$H = -\frac{\hbar^2}{2m} \frac{d^2}{dz^2} + V(z). \quad (1)$$

Introducing inverse temperature $\beta = 1/(k_B T)$ with Boltzmann constant k_B , we define the Gibbs operator

$$\rho = \exp[-\beta H], \quad (2)$$

the matrix elements of which define the so-called density matrix $\rho(x, y, \beta) = \langle x | \rho | y \rangle$. The partition function

$$Z(\beta) = \text{Trace} [\rho] = \int_{-\infty}^{+\infty} dz \rho(z, z, \beta) \quad (3)$$

is well behaved thanks to the confining nature of potential V (in other words, integral over z does converge because $\rho(z, z, \beta)$ decays sufficiently fast at large distances). The (normalized) probability density to find the particle at position x then reduces to

$$\Psi(x, \beta) = \frac{\rho(x, x, \beta)}{Z(\beta)}. \quad (4)$$

For further purposes, it is also convenient to introduce the spectral representations of density matrix and partition function, which read

$$\rho(x, y, \beta) = \sum_{k=0}^{+\infty} \phi_k(x) \phi_k^*(y) \exp(-\beta E_k) \quad (5)$$

and

$$Z(\beta) = \sum_{k=0}^{+\infty} \exp(-\beta E_k). \quad (6)$$

In such representations, E_k is the k -th eigenvalue of H , while ϕ_k is its associated eigenfunction which satisfies Schrödinger equation

$$\left[-\frac{\hbar^2}{2m} \frac{d^2}{dz^2} + V(z)\right] \phi_k(z) = E_k \phi_k(z). \quad (7)$$

B. Feynman-Kac formula

Path integrals were first introduced for representing the matrix elements of the evolution operator $\exp(-iHt/\hbar)$ associated with Schrödinger equation [1]. It was soon realized that a similar path integral representation for matrix elements of Gibbs operator at inverse temperature β can be inferred via the formal substitution $t \rightarrow -i\beta\hbar$. The latter representation for $\rho(x, y, \beta)$ involves an integral over all paths $\omega(\cdot)$ going from $\omega(0) = x$ to $\omega(\beta\hbar) = y$ in a time $\beta\hbar$. Moreover, the corresponding integrand is the exponential factor $\exp[-S(\omega(\cdot))/\hbar]$, where $S(\omega(\cdot))$ is the action associated with path $\omega(\cdot)$. That path integral is proved to be mathematically well defined for a large class of potentials. Its convergence is indeed ensured, roughly speaking, by the Gaussian-like decay of the kinetic part of $\exp[-S(\omega(\cdot))/\hbar]$ for large paths (on the contrary, path integrals for $\exp(-iHt/\hbar)$ are, in general, ill-defined because they involve sums of oscillating phase factors).

The genuine path integral representation of $\rho(x, y, \beta)$ can be rewritten within the parametrization $\omega(u) = (1-s)x + sy + \lambda_D \xi(s)$, where $s = u/(\beta\hbar)$ is the dimensionless time in $\beta\hbar$ units, while $\xi(s)$ is a Brownian bridge satisfying boundary conditions $\xi(0) = \xi(1) = 0$ and $\lambda_D = (\beta\hbar^2/m)^{1/2}$ is the de Broglie wavelength. On the one hand, the kinetic part of $\exp[-S(\omega(\cdot))/\hbar]$ then provides normalized Wiener measure $\mathcal{D}_W(\xi)$ associated with the Brownian bridge process. That Gaussian measure is entirely defined by its first two moments

$$\int_{\Omega} \mathcal{D}_W(\xi) \xi(s) = 0, \quad (8)$$

$$\int_{\Omega} \mathcal{D}_W(\xi) \xi(s_1) \xi(s_2) = \min(s_1, s_2) (1 - \max(s_1, s_2)). \quad (9)$$

On the other hand, the potential part of $\exp[-S(\omega(\cdot))/\hbar]$ reduces to the Boltzmann factor associated with time average of V along path $(1-s)x + sy + \lambda_D \xi(s)$. The resulting so-called Feynman-Kac formula reads [2]

$$\rho(x, y, \beta) = \frac{\exp[-(x-y)^2/(2\lambda_D^2)]}{\sqrt{2\pi}\lambda_D} \int_{\Omega} \mathcal{D}_W(\xi) \exp\left(-\beta \int_0^1 ds V((1-s)x + sy + \lambda_D \xi(s))\right) \quad (10)$$

where $\Omega = \{\xi(\cdot)\}$ is the infinite set of realizations of the Brownian bridge process.

In the Feynman-Kac formula (10), the Wiener measure is intrinsic to Brownian motion and does not depend on any physical parameter. Expression (9) of the covariance implies that the typical extension of a Brownian bridge is always of order 1. Mass m of the particle, as well as Planck's constant \hbar only intervene in the de Broglie wavelength λ_D . That length controls the size of quantum fluctuations, as shown by specifying (10) to diagonal elements, i.e.

$$\rho(x, x, \beta) = \frac{1}{\sqrt{2\pi}\lambda_D} \int_{\Omega} \mathcal{D}_W(\xi) \exp\left(-\beta \int_0^1 ds V(x + \lambda_D \xi(s))\right). \quad (11)$$

In time-average $\int_0^1 ds V(x + \lambda_D \xi(s))$, particle experiences the potential around position x on a length scale obviously determined by λ_D , as illustrated in Figure 1.

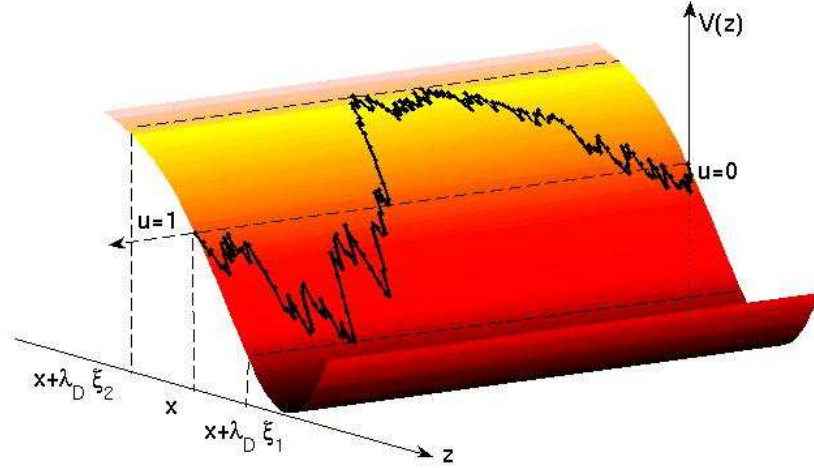


FIG. 1: Typical path which starts and ends at position x , along which particle experiences potential V . Dashed lines indicate the two edges of a fictitious box determined by the extremal deviations ξ_1 and ξ_2 of the path. Typical sizes of ξ_1 and ξ_2 are controlled by λ_D

Besides its interest for analytical or numerical calculations (see below), Feynman-Kac representation is also quite useful for mapping a quantum system into a classical one [12, 13, 14]. Indeed, formula (11) can be reinterpreted in terms of a classical extended object, often called loop or polymer, defined by its position x and its internal shape parametrized by $\lambda_D \xi(\cdot)$. Then, the r.h.s. of (11) is nothing but the statistical average of a Boltzmann factor for the loop over its all possible shapes distributed according to Wiener measure. That interpretation, which holds for any quantum system with an arbitrary number of particles, is the key starting point of above mapping.

C. High and finite temperatures

At high temperatures, the de Broglie wavelength is small, so only paths which remain close to reference position x contribute significantly to $\rho(x, x, \beta)$ in (11). Therefore, the time-average of V along path $x + \lambda_D \xi(s)$ can be performed by replacing $V(x + \lambda_D \xi(s))$ by its Taylor series around $V(x)$

$$V(x + \lambda_D \xi(s)) = V(x) + \sum_{n=1}^{\infty} \frac{(\lambda_D \xi(s))^n}{n!} \frac{d^n V}{dx^n} \quad (12)$$

(we assume that V is infinitely differentiable). If we keep only the first term in (12), which does not depend on $\xi(s)$, we immediately recover the familiar classical form of $\rho(x, x, \beta)$

$$\frac{1}{\sqrt{2\pi\lambda_D}} \exp[-\beta V(x)], \quad (13)$$

where we have used normalization condition $\int_{\Omega} \mathcal{D}_W(\xi) = 1$. Since λ_D is proportional to \hbar , quantum corrections to (13) are easily generated by a (formal) cumulant expansion of contributions associated with terms $n \geq 1$ in (12). The resulting moments of Wiener measure are then readily computed by Wick's theorem which applies thanks to Gaussian character of $\mathcal{D}_W(\xi)$. This allows us to retrieve the well-known Wigner-Kirkwood expansion in powers of \hbar^2

$$\rho(x, x, \beta) = \frac{e^{-\beta V(x)}}{\sqrt{2\pi\lambda_D}} \left[1 - \frac{\beta^2 \hbar^2}{12m} \frac{d^2 V}{dx^2} + \frac{\beta^3 \hbar^2}{24m} \left(\frac{dV}{dx} \right)^2 + \dots \right]. \quad (14)$$

Expansion (14) involves only even powers of \hbar , because all odd moments of gaussian Wiener measure vanish by virtue of (8). That expansion is expected to be only asymptotic. Present derivation within FK representation turns out to be much easier than usual approaches within Wigner-distribution formalism (see e.g ref. [6]). It might be used

for calculating higher-order terms beyond \hbar^2 -correction (terms up to order \hbar^6 have been already determined in the literature [15]). Moreover, it clearly emphasizes that (14) is appropriate when the de Broglie wavelength is much smaller than the typical length of variation of the potential. Then, truncation of (14) up to a few terms should provide accurate values of the density matrix, as checked below.

When the temperature decreases, the de Broglie wavelength increases, so Wigner-Kirkwood expansion is no longer applicable. At the analytical level, exact evaluations of the corresponding path integrals are not accessible in general, except for some simple models [3]. Non-perturbative effects in \hbar can be partially accounted for through various methods, among which the celebrated semi-classical approximation described further. The reliability of such methods remains questionable since they do not involve any small control-parameter like (14). Nonetheless, for numerical purposes, their accuracy may be satisfactory, at least at not too low temperatures.

If analytic informations on the density matrix become rather difficult to extract from FK representation, accurate values can be still readily obtained at finite temperatures *via* direct numerical estimations of FK path integrals. A first possible route starts with the (exact) convolution relation

$$\rho(x, x, \beta) = \int \prod_{i=1}^N dz_i \prod_{i=0}^N \rho(z_i, z_{i+1}, \beta/(N+1)) \quad (15)$$

with $z_0 = z_{N+1} = x$. For a sufficiently large value of N , each matrix element $\rho(z_i, z_{i+1}, \beta/(N+1))$ can be evaluated within FK formula (10) by neglecting the corresponding Brownian deviation $\lambda_D \xi(s)/(N+1)^{1/2}$ in the argument of V . The resulting time average $\int_0^1 ds V((1-s)x + sy)$ can be itself replaced, with a similar accuracy, by $V((x+y)/2)$ (middle-point convention) for instance. The resulting approximate expression

$$\int \prod_{i=1}^N dz_i \prod_{i=0}^N \frac{\exp[-(N+1)(z_i - z_{i+1})^2/(2\lambda_D^2)]}{\sqrt{2\pi\lambda_D/(N+1)^{1/2}}} \exp[-(\beta/(N+1)) \sum_{i=0}^N V((z_i + z_{i+1})/2)] \quad (16)$$

turns out to be quite accurate for rather small values of N , provided that $\lambda_D/(N+1)^{1/2}$ is smaller than the typical length of variation of the potential. We stress that (16) becomes exact when $N \rightarrow \infty$. In fact, continuous path integration with Wiener measure may be precisely defined in the framework of that limit process.

A second route for direct numerical computations relies on the introduction of a set of N simple functions $e_n(s)$ ($n = 1 \dots N$) with $e_n(0) = e_n(1) = 0$, such that they define a basis for Brownian bridges $\xi(s)$ in the limit $N \rightarrow \infty$ [9]. Numerical evaluations of (11) are then carried out by replacing the functional integration over paths by ordinary integrals over coefficients a_n arising in the decomposition $\xi(s) = a_n e_n(s)$. That method provides satisfactory results by using only a few number N of basis functions [9]. Similarly to the previous convolution method, it becomes exact when $N \rightarrow \infty$.

D. Low temperatures

When temperature goes to zero, λ_D diverges, so most paths explore a rather large region not restricted to the neighbourhood of reference position x . A direct analysis of FK expression (11) then becomes quite cumbersome. In particular, $\rho(x, x, \beta)$ must behave as

$$\rho(x, x, \beta) \stackrel{\beta \rightarrow +\infty}{\sim} |\phi_0(x)|^2 \exp[-\beta E_0], \quad (17)$$

which immediately follows from spectral representation of density matrix (5). Indeed, the groundstate obviously provides the leading contribution in the r.h.s. of (5). The factorization of position and temperature dependences in (17) does not come out easily from FK formula (11), where both position and temperature are coupled in an absolutely non-trivial way. By the way, notice that spectral representation (5) is not well suited at intermediate or high temperatures, because one has then to sum a large number of contributions associated with various eigenstates (in particular, classical behaviour (13) cannot be straightforwardly recovered by using (5)).

When temperature becomes too small, previous computational methods become more difficult to handle accurately. Even if some algorithmic tricks [16] may significantly reduce calculation-times within a satisfactory accuracy, they do not provide a better understanding of low-temperature behaviours.

III. BOX FORMULA

A. The central observations

Let us consider a symmetric confining potential $V(z)$ with a minimum located at $z = 0$. On the one hand, low-temperature behaviour (17) of the corresponding density matrix is mainly determined by the local shape of $V(z)$ over finite length scale a_0 , which characterizes the spatial extension of the groundstate wave function $\phi_0(x)$. On the other hand, for typical paths with size of order λ_D , time-average potential $\int_0^1 ds V(x + \lambda_D \xi(s))$ becomes, roughly speaking, of order $\int_0^{\lambda_D} dz V(z) / \lambda_D$ when λ_D is sufficiently large. At low temperatures, their contribution to the r.h.s. of (11) is then controlled by the large-distance behaviour of $V(z)$. Thus, low-temperature behaviour (17) is not provided by typical paths. That argument can be implemented through semi-quantitative estimations for specific cases. If $V(z)$ diverges as $|z|^n$ ($n > 0$), contributions of typical paths to (11) behave (discarding multiplicative powers of β) as $\exp[-c(\beta)^{1+n/2}]$ with some positive constant c : they are exponentially smaller than leading Boltzmann factor $\exp[-\beta E_0]$.

The previous analysis suggests that, at low temperatures, leading contributions to the r.h.s. of (11) arise from paths with a spatial extension of order a_0 , i.e. from quite small Brownian bridges with size $|\xi(s)|$ of order a_0/λ_D . For such paths, time-average potential $\int_0^1 ds V(x + \lambda_D \xi(s))$ is of order $V(a_0)$, so the corresponding Boltzmann factor indeed is of order $\exp[-\beta E_0]$. Notice that, paths with very different shapes give raise to similar contributions, since the Wiener weights of the associated Brownian bridges remain of order (roughly speaking) $\exp(-\int_0^1 ds (\dot{\xi}(s))^2/2) \sim \exp(-a_0^2/\lambda_D^2) \sim 1$. Consequently, when the temperature decreases, only a very tiny subset of paths gives a relevant contribution to the r.h.s. of (11). In other words, important paths are not any more typical but, on the contrary, they can be viewed as large deviations. This explains why direct numerical evaluations of (11) become rather difficult: the subset of important paths remains, in some sense, hidden in the entire configurational space.

In order to extract from (11) the relevant contributions at low temperatures, it is tempting to collect all paths with the same finite spatial extension, and then to sum over all possible extensions. That procedure is not easy to carry out directly in the r.h.s. of (11), within a suitable partition of functional integration space over Brownian bridges. As described below, it is more convenient to transform first the density matrix within the operator representation, by introducing an auxiliary Hamiltonian which confines the particle inside a box with size ℓ .

B. The auxiliary Hamiltonian approach

Let us introduce the auxiliary Hamiltonian

$$H_\ell = H^0 + V + V_\ell, \quad (18)$$

where H^0 denotes the kinetic Hamiltonian. The additional potential V_ℓ is defined by

$$V_\ell(z) = V_0 [1 - \Theta(z + \ell) + \Theta(z - \ell)], \quad (19)$$

where Θ is the Heavyside function, while V_0 denotes barrier height ($V_0 > 0$). That potential tends to confine the particle inside a box with extension ℓ . Expression (18) reduces to Hamiltonian (1) when ℓ goes to infinity. In that limit, for x kept fixed, diagonal part $\langle x | \rho_\ell | x \rangle$ of density matrix $\rho_\ell = \exp[-\beta H_\ell]$ goes to $\langle x | \rho | x \rangle$.

The identity,

$$\langle x | \rho | x \rangle = \langle x | \rho_L | x \rangle + \int_L^\infty d\ell \langle x | \partial_\ell [\rho_\ell] | x \rangle \quad (20)$$

which is valid for any reference extension L and for any height V_0 of the confining potential is quite useful for our purpose. We set $L = |x|$, and we consider an infinitely high potential barrier V_0 . Under that limit, the contact density goes to zero,

$$\lim_{V_0 \rightarrow +\infty} \langle x | \rho_{|x|} | x \rangle = 0, \quad (21)$$

because the probability for the particle to stay on the boundary vanishes for infinitely high walls. Thus, identity (20) is rewritten as

$$\langle x|\rho|x\rangle = \lim_{V_0 \rightarrow \infty} \int_{|x|}^{\infty} d\ell \langle x|\partial_\ell [\rho_\ell]|x\rangle. \quad (22)$$

The right hand side can be transformed by applying Dyson formula

$$\partial_\ell \left[e^{-A(\ell)} \right] = - \int_0^1 ds e^{-[1-s]A(\ell)} \partial_\ell [A(\ell)] e^{-sA(\ell)}, \quad (23)$$

valid for any operator $A(\ell)$ which depends on ℓ . This provides

$$\partial_\ell [\rho_\ell] = -\beta \int_0^1 ds \int_{-\infty}^{+\infty} dz e^{-\beta(1-s)H_\ell} |z\rangle \langle z| \partial_\ell [H_\ell] e^{-\beta s H_\ell} \quad (24)$$

$$= \beta V_0 \int_0^1 ds \int_{-\infty}^{+\infty} dz e^{-\beta(1-s)H_\ell} |z\rangle [\delta(z-\ell) + \delta(z+\ell)] \langle z| e^{-\beta s H_\ell} \quad (25)$$

$$= \beta V_0 \int_0^1 ds \left(e^{-\beta(1-s)H_\ell} |\ell\rangle \langle \ell| e^{-\beta s H_\ell} + e^{-\beta(1-s)H_\ell} |-\ell\rangle \langle -\ell| e^{-\beta s H_\ell} \right), \quad (26)$$

from which we infer

$$\rho(x, x, \beta) = \lim_{V_0 \rightarrow \infty} \beta V_0 \int_{|x|}^{\infty} d\ell \int_0^1 ds [\rho_\ell(x, \ell, \beta[1-s]) \rho_\ell(\ell, x, \beta s) + \rho_\ell(x, -\ell, \beta[1-s]) \rho_\ell(-\ell, x, \beta s)]. \quad (27)$$

That expression must be considered with some caution because when V_0 diverges the different integrands vanishes. Therefore, additional work is necessary to control limit $V_0 \rightarrow \infty$.

For that purpose, we rewrite the integrands in terms of constrained density matrix ρ_ℓ^0 of the *free* particle submitted to confining potential V_ℓ . According to the obvious equality

$$\rho_\ell(x_i, x_f, \beta) = \rho_\ell^0(x_i, x_f, \beta) \frac{\rho_\ell(x_i, x_f, \beta)}{\rho_\ell^0(x_i, x_f, \beta)}, \quad (28)$$

and since ρ_ℓ/ρ_ℓ^0 remains finite when $V_0 \rightarrow \infty$, we define

$$g^\pm(x, \ell, s, \beta) = \lim_{V_0 \rightarrow \infty} (2\pi)^{1/2} \lambda_D (\beta V_0) \rho_\ell^0(x, \pm\ell, \beta s) \rho_\ell^0(\pm\ell, x, \beta(1-s)). \quad (29)$$

After using Feynman-Kac formula for both ρ_ℓ and ρ_ℓ^0 in ratio ρ_ℓ/ρ_ℓ^0 , we transform (27) into

$$\begin{aligned} \rho(x, x, \beta) &= \int_{|x|}^{+\infty} d\ell \int_0^1 ds \frac{g^-(x, \ell, s, \beta)}{\sqrt{2\pi\lambda_D}} \left\langle \exp \left[-\beta s \int_0^1 du V(z(u)) \right] \right\rangle_{\Omega_s^-} \left\langle \exp \left[-\beta(1-s) \int_0^1 du V(z(u)) \right] \right\rangle_{\Omega_{1-s}^-} \\ &+ \int_{|x|}^{+\infty} d\ell \int_0^1 ds \frac{g^+(x, \ell, s, \beta)}{\sqrt{2\pi\lambda_D}} \left\langle \exp \left[-\beta s \int_0^1 du V(z(u)) \right] \right\rangle_{\Omega_s^+} \left\langle \exp \left[-\beta(1-s) \int_0^1 du V(z(u)) \right] \right\rangle_{\Omega_{1-s}^+} \end{aligned} \quad (30)$$

Notation $\langle \cdot \rangle_\omega$ denotes an average over a constrained Brownian process which belongs to a set ω . Paths $z(u)$ are expressed in terms of Brownian bridges according to $z(u) = x(1-u) \pm u\ell + \sqrt{s}\lambda_D \xi(u)$ for Ω_s^\pm . Moreover those paths must stay inside the box $[-\ell, +\ell]$, so that constraint defines the corresponding sets Ω_s^\pm . The statistical weight of a path in such a constrained average is its associated Wiener measure $\mathcal{D}_W(\xi)$. For the sake of notational convenience, we do not explicitly write the dependences on both x and ℓ of Ω_s^\pm .

The physical interpretation of functions g^\pm clearly emerges from (30), if we specify that general formula to the particular case $V(z) = 0$. Such functions are the (normalized) statistical weights of the constrained sets $\Omega^\pm = \Omega_s^\pm \cup \Omega_{1-s}^\pm$, *i.e.* the sum of statistical weights of all paths touching the boundaries of the box at time s (see Figure 2). Therefore, in the following, we set $g^\pm(x, \ell, s, \beta) = g(\Omega^\pm)$. Analytical calculations of those weights are performed in Appendix A, by using the spectral representation of ρ_ℓ^0 .

The first step of our rewriting of Feynman-Kac representation, is achieved through formula (30). Paths are indeed collected together according to their extension $\pm\ell$. Notice that the touching time, s , is also crucial for defining the corresponding proper partition of the genuine integration space over all unconstrained paths.

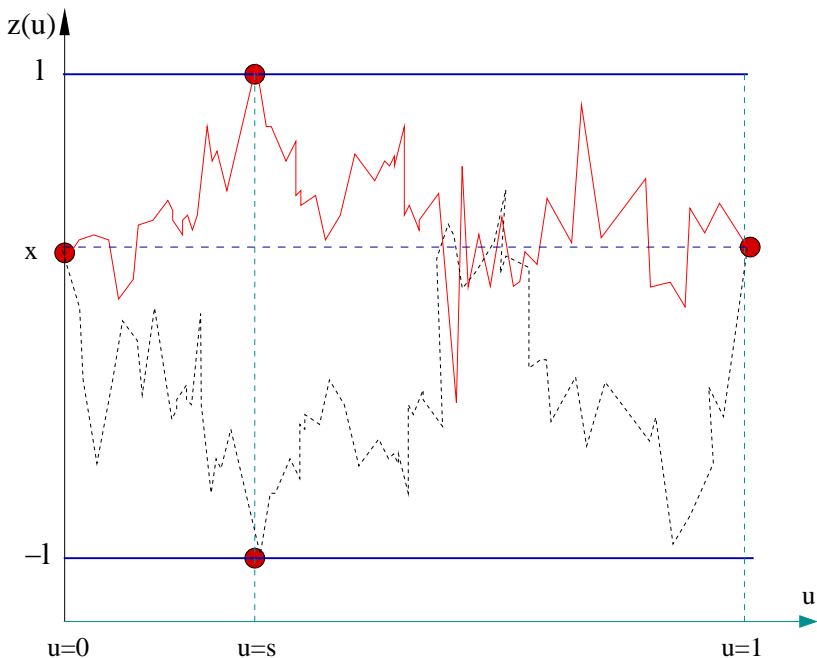


FIG. 2: Typical paths which start and end at position x . Solid and dashed lines represent paths which belong to Ω^+ and to Ω^- respectively.

C. Introduction of averages over occupation times

In a second step, we introduce the so-called *occupation time*, defined for each given path $z(u)$ in Ω_s^\pm by

$$\theta_z(x') = \int_0^1 du \delta(x' - z(u)). \quad (31)$$

The quantity $\theta_z(x')dx'$ is the total time passed in a neighborhood dx' of position x' by the particle when it follows Brownian path $z(u)$. Of course, the total time passed in the whole box is always equal to 1, *i.e.*

$$\int_{-\ell}^{+\ell} dx' \theta_z(x') = 1. \quad (32)$$

Time-averaged potential along path $z(u)$ is then expressed in terms of occupation time via the obvious identity

$$\int_0^1 du V(z(u)) = \int_{-\ell}^{+\ell} dx' \theta_z(x') V(x'), \quad (33)$$

valid for any path $z(u)$.

According to identity (33), Boltzmann factors involved in averages

$$\left\langle \exp \left[-\beta s \int_0^1 du V(z(u)) \right] \right\rangle_{\Omega_s^\pm}, \quad (34)$$

only depend on the occupation time $\theta_z(x')$. As illustrated in Fig. 3, various different paths may provide the same occupation time. As quoted in Section III A, their statistical weights are close together, so their contributions to average (34) are almost identical. Thus, it is now tempting to collect all paths which provide the same occupation time $\theta(x')$, via the introduction of the corresponding density measure $\mathcal{D}_{\Omega_s^\pm}[\theta]$. After expressing averages (34) over

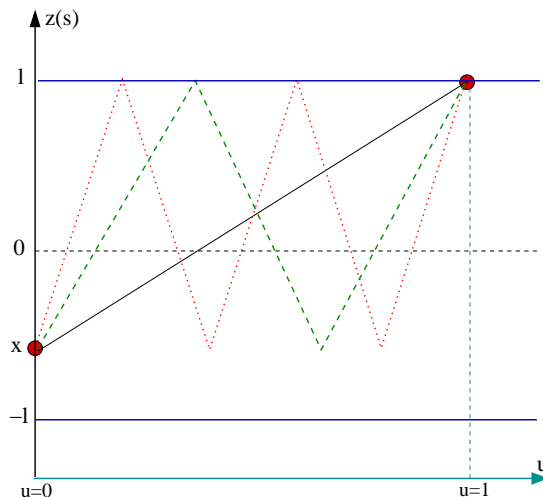


FIG. 3: Three different paths which start at x and end at $+l$, while the corresponding occupation times are identical.

constrained paths, as averages over occupation times with (normalized) measure $\mathcal{D}_{\Omega_s^\pm}[\theta]$, we eventually obtain the box formula

$$\begin{aligned} \rho(x, x, \beta) = & \int_{|x|}^{+\infty} d\ell \int_0^1 ds \frac{g(\Omega^-)}{\sqrt{2\pi\lambda_D}} \int \mathcal{D}_{\Omega_s^-}[\theta] \exp\left[-\beta s \int_{-\ell}^{+\ell} dx' \theta(x') V(x')\right] \int \mathcal{D}_{\Omega_{1-s}^-}[\theta] \exp\left[-\beta(1-s) \int_{-\ell}^{+\ell} dx' \theta(x') V(x')\right] \\ & + \int_{|x|}^{+\infty} d\ell \int_0^1 ds \frac{g(\Omega^+)}{\sqrt{2\pi\lambda_D}} \int \mathcal{D}_{\Omega_s^+}[\theta] \exp\left[-\beta s \int_{-\ell}^{+\ell} dx' \theta(x') V(x')\right] \int \mathcal{D}_{\Omega_{1-s}^+}[\theta] \exp\left[-\beta(1-s) \int_{-\ell}^{+\ell} dx' \theta(x') V(x')\right]. \end{aligned} \quad (35)$$

If statistical weights $g(\Omega^\pm)$ are analytically known (see Appendix A), explicit expressions for density measures $\mathcal{D}_{\Omega_s^\pm}[\theta]$ are not available. Such probability densities result from the summation of Wiener measures over all Brownian paths inside Ω_s^\pm which provide the same occupation time. That procedure is quite difficult to handle in closed analytical forms, and only the moments of $\mathcal{D}_{\Omega_s^\pm}[\theta]$ can be computed explicitly. Nevertheless, box formula (35) turns out to be quite useful for various purposes, as suggested by the following simple comments and arguments.

Contrary to the case of the genuine Feynman-Kac representation, leading contributions at low temperature merely emerge from box formula (35). Indeed, for x of order a_0 , boxes with size ℓ of order a few a_0 do provide contributions of order $\exp(-\beta E_0)$, because weight factors $g(\Omega^\pm)$ are of order $\exp(-\beta \hbar^2 / (2m\ell^2))$ for $\ell \ll \lambda_D$ (see Appendix A), while products of averages of Boltzmann factors over occupation times are of order $\exp(-\beta \int_0^\ell dx' V(x') / \ell)$. That rough analysis will be implemented in a forthcoming paper, where we show more precisely how low temperature behaviour (17) arises from scaling properties of distributions $\mathcal{D}_{\Omega_s^\pm}[\theta]$ in the regime $\ell \ll \lambda_D$.

If Brownian paths are quite noisy, the corresponding occupation times may have rather regular shapes. This is illustrated in Fig. 4a, which shows a regular path on the one hand, and a very jagged one on the other hand: both paths provide occupation times with regular shapes displayed in Fig. 4b (notice that the corresponding contributions to Boltzmann factors are of course different). That observation leads to a first type of approximations based on simple modelizations of distributions $\mathcal{D}_{\Omega_s^\pm}[\theta]$ within restricted sets of elementary functions which represent the various occupation times (they will be described elsewhere). A second type of approximations is based on the truncation of cumulant expansions, where key ingredients do exhibit regular behaviours with respect to spatial positions. One of them is presented further in Section IV.

Eventually, notice that box formula (35) can be immediately extended to any potential $V(x)$, not necessarily confining. Similar formula can be derived in higher dimensions or for systems with more than one particle. Those various extensions may include different box shapes or different confining potentials $V_0(x)$.

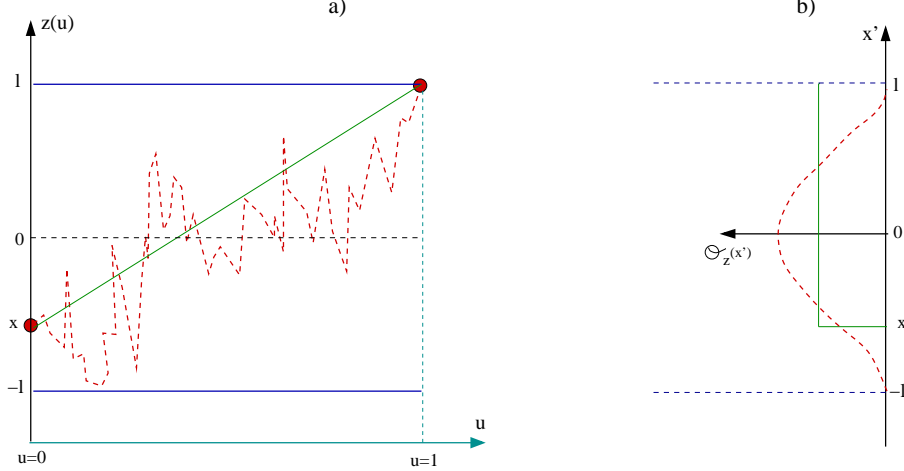


FIG. 4: Panel (a) presents two different paths which start at position x at time $u = 0$ and end at ℓ for time $u = 1$. Panel (b) shows their corresponding occupation times $\theta_z(x')$.

IV. ERGODIC APPROXIMATION

A. Truncation of the cumulant expansion

Formally, averages over distributions $\mathcal{D}_{\Omega_s^\pm}[\theta]$ involved in the r.h.s. of box formula (35) can be represented by their infinite cumulant expansions. A natural approximation consists in truncating that expansion up to its first term, *i.e.* we replace the averages

$$\int \mathcal{D}_{\Omega_s^\pm}[\theta] \exp\left[-\beta s \int_{-\ell}^{+\ell} dx' \theta(x') V(x')\right] \quad (36)$$

by

$$\exp\left(-\beta s \int_{-\ell}^{+\ell} dx' \langle \theta(x') \rangle_{\Omega_s^\pm} V(x')\right). \quad (37)$$

We call that lowest order approximation *ergodic*, since it would be exact if paths were experiencing all parts of the potential with a probability independent of time. It amounts to replace (imaginary) time averages of the potential by spatial averages with a measure defined by mean occupation-time

$$\langle \theta(x') \rangle_{\Omega_s^\pm} = \int \mathcal{D}_{\Omega_s^\pm}[\theta] \theta(x'). \quad (38)$$

Inserting (37) into (35), we obtain the subsequent ergodic approximation for density matrix,

$$\begin{aligned} \rho_{erg}(x, x, \beta) &= \int_{|x|}^{+\infty} d\ell \int_0^1 ds \frac{g(\Omega^-)}{\sqrt{2\pi\lambda_D}} \exp\left[-\beta \int_{-\ell}^{+\ell} dx' \left(s \langle \theta(x') \rangle_{\Omega_s^-} + [1-s] \langle \theta(x') \rangle_{\Omega_{1-s}^-}\right) V(x')\right] \\ &+ \int_{|x|}^{+\infty} d\ell \int_0^1 ds \frac{g(\Omega^+)}{\sqrt{2\pi\lambda_D}} \exp\left[-\beta \int_{-\ell}^{+\ell} dx' \left(s \langle \theta(x') \rangle_{\Omega_s^+} + [1-s] \langle \theta(x') \rangle_{\Omega_{1-s}^+}\right) V(x')\right]. \end{aligned} \quad (39)$$

B. Mean occupation time in terms of Brownian Green functions

The average occupation time can be obtained within two different methods: either by using operator algebra (see Appendix B) or, in a more physical way, by using Brownian motion properties, as shown below. First we compute

the mean occupation time around position x' , over Brownian paths at inverse temperature β' which start from x_i at time $u = 0$ and end at x_f for time $u = 1$. Those Brownian paths are constrained within the interval $[-\ell, +\ell]$, and they define a set $\omega = \{z(u) = x_i(1-u) + x_f u + \lambda \xi(u)\}$ with $\lambda^2 = \beta' \hbar^2 / m$.

Introducing the constrained probability density $f_\omega(z, u)$ to find the Brownian particle at the position z for time u , the mean occupation time reads

$$\langle \theta(x') \rangle_\omega = \int_0^1 du f_\omega(x', u). \quad (40)$$

The probability density $f_\omega(x', u)$ can be generated by using the Green function $G_\omega(z, t|z_0, t_0)$ of the diffusion equation, solved with Dirichlet boundary conditions $G_\omega(\pm\ell, t|z_0, t_0) = 0$ and initial condition $G_\omega(z, t_0|z_0, t_0) = \delta(z - z_0)$. That Green function reduces to

$$G_\omega(z, t|z_0, t_0) = \frac{1}{\ell} \sum_{n=1}^{\infty} \psi_n(z_0/\ell) \psi_n(z/\ell) \exp \left[-(t - t_0) \frac{\lambda^2 \pi^2}{\ell^2} n^2 \right], \quad (41)$$

with $\psi_n(z/\ell) = \sin [n\pi(z + \ell)/(2\ell)]$. Since Brownian motion is a Markov process, the constrained probability density $f_\omega(x', u)$ is then

$$f_\omega(x', u) = \frac{G_\omega(x', u|x_i, 0) G_\omega(x_f, 1-u|x', 0)}{G_\omega(x_f, 1|x_i, 0)}. \quad (42)$$

Now, we focus on the specific case $\omega = \Omega_s^-$ (i.e. $x_f = -\ell$, $x_i = x$ and $\beta' = \beta s$). According to (41), the Green function $G_{\Omega_s^-}(x', u|x, 0)$ can be rewritten as

$$G_{\Omega_s^-}(x', u|x, 0) = \frac{1}{\ell} \eta_1 \left(\frac{x}{\ell}, \frac{x'}{\ell}, \frac{\lambda_D \sqrt{s}}{\ell}, u \right), \quad (43)$$

where η_1 is a dimensionless function depending on four dimensionless variables. Similarly, we find

$$\frac{G_{\Omega_s^-}(-\ell, 1-u|x', 0)}{G_{\Omega_s^-}(-\ell, 1|x, 0)} = \eta_2 \left(\frac{x}{\ell}, \frac{x'}{\ell}, \frac{\lambda_D \sqrt{s}}{\ell}, u \right). \quad (44)$$

If we introduce the dimensionless function Φ defined as

$$\Phi(\alpha', \alpha, y) = \int_0^1 du \eta_1(\alpha, \alpha', y, u) \eta_2(\alpha, \alpha', y, u), \quad (45)$$

we obtain

$$\langle \theta(x') \rangle_{\Omega_s^-} = \frac{1}{\ell} \Phi \left(\frac{x}{\ell}, \frac{x'}{\ell}, \frac{\lambda_D \sqrt{s}}{\ell} \right). \quad (46)$$

Furthermore, thanks to the symmetry properties of Green functions, $G_\omega(z, t|z_0, t_0) = G_\omega(z_0, t|z, t_0) = G_\omega(-z, t| -z_0, t_0)$, $\langle \theta(x') \rangle_{\Omega_s^+}$ is also given by

$$\langle \theta(x') \rangle_{\Omega_s^+} = \frac{1}{\ell} \Phi \left(\frac{-x}{\ell}, \frac{-x'}{\ell}, \frac{\lambda_D \sqrt{s}}{\ell} \right). \quad (47)$$

Inserting those expressions of mean occupation times for various sets Ω_s^\pm into (39), the ergodic form of the density matrix is rewritten as

$$\begin{aligned} \rho_{erg}(x, x, \beta) &= \int_{|x|}^{+\infty} d\ell \int_0^1 ds \frac{g(x, \ell, s, \beta)}{\sqrt{2\pi\lambda_D}} \exp \left(-\beta \int_{-1}^1 d\alpha' \left[s\Phi \left(\frac{x}{\ell}, \alpha', \frac{\pi\lambda_D\sqrt{s}}{2\ell} \right) + [1-s]\Phi \left(\frac{x}{\ell}, \alpha', \frac{\pi\lambda_D\sqrt{1-s}}{2\ell} \right) \right] V(\alpha'\ell) \right) \\ &+ \int_{|x|}^{+\infty} d\ell \int_0^1 ds \frac{g(-x, \ell, s, \beta)}{\sqrt{2\pi\lambda_D}} \exp \left(-\beta \int_{-1}^1 d\alpha' \left[s\Phi \left(\frac{-x}{\ell}, \alpha', \frac{\pi\lambda_D\sqrt{s}}{2\ell} \right) + [1-s]\Phi \left(\frac{-x}{\ell}, \alpha', \frac{\pi\lambda_D\sqrt{1-s}}{2\ell} \right) \right] V(-\alpha'\ell) \right) \end{aligned} \quad (48)$$

with $g(x, \ell, s, \beta) = g(\Omega_s^-)$. In (48), all quantities are explicitly known in terms of simple series involving Gaussian and trigonometric functions. Box weight $g(x, \ell, s, \beta)$ is computed in Appendix A, while a similar expression is derived for Φ in the next subsection (see formula (52)). Within the ergodic approximation, we are left with the evaluation of two ordinary integrals, which is of course much easier than a direct evaluation of the genuine functional integrals.

C. Analytical estimations for Φ at low and high temperatures

1. General expression for Φ

First, we derive a general expression for Φ , valid at any temperature. The spectral expressions of η_1 and η_2 are

$$\eta_1(\alpha, \alpha', y, u) = \sum_{n=1}^{\infty} \psi_n(\alpha) \psi_n(\alpha') \exp\left[-\frac{y^2}{2} n^2 u\right], \quad (49)$$

$$\eta_2(\alpha, \alpha', y, u) = \frac{\sum_{n=1}^{\infty} \psi_n(\alpha') n \exp\left[-\frac{y^2}{2} n^2 [1-u]\right]}{\sum_{n=1}^{\infty} \psi_n(\alpha) n \exp\left[-\frac{y^2}{2} n^2\right]}. \quad (50)$$

Inserting those expressions into formula (45), we find the general expression for Φ ,

$$\Phi(\alpha, \alpha', y) = \frac{\sum_{n=1}^{\infty} \psi_n(\alpha) \psi_n^2(\alpha') n \exp\left[-\frac{y^2}{2} n^2\right] + \frac{2}{y^2} \sum_{n \neq k, 1}^{\infty} \psi_n(\alpha) \psi_n(\alpha') \psi_k(\alpha') k \frac{\exp\left[-\frac{y^2}{2} n^2\right] - \exp\left[-\frac{y^2}{2} k^2\right]}{k^2 - n^2}}{\sum_{n=1}^{\infty} \psi_n(\alpha) n \exp\left[-\frac{y^2}{2} n^2\right]}. \quad (51)$$

Normalization condition $\int_{-1}^{+1} \Phi(\alpha, \alpha', y) = 1$, which follows from (32), is indeed satisfied by (51) thanks to the orthogonality of the ψ_n 's, *i.e.* $\int_{-1}^{+1} dx \psi_n(x) \psi_k(x) = \delta_{k,n}$. Within simple algebra, that last expression can be rewritten as a simple sum [17]

$$\Phi(\alpha, \alpha', y) = \frac{\sum_{n=1}^{\infty} \exp\left[-\frac{y^2}{2} n^2\right] \psi_n(\alpha') \left[n \psi_n(\alpha) \psi_n(\alpha') + \frac{2}{y^2} A_n(\alpha, \alpha')\right]}{\sum_{n=1}^{\infty} \psi_n(\alpha) n \exp\left[-\frac{y^2}{2} n^2\right]}, \quad (52)$$

with

$$A_n(\alpha, \alpha') = \frac{\pi}{8} \left[(1 - \alpha - 2\alpha') \sin\left[n \frac{\pi}{2} (\alpha + \alpha' + 2)\right] + \left(1 + \alpha - 2\alpha' - 2 \frac{\alpha - \alpha'}{|\alpha - \alpha'}\right) \sin\left[n \frac{\pi}{2} (\alpha - \alpha')\right] \right]. \quad (53)$$

In formula (48), third variable y of the function Φ is proportional to λ_D/ℓ . Thus the low and high temperature regimes correspond to the limits $y \rightarrow \infty$ and $y \rightarrow 0$ respectively. In the next subsections, we derive asymptotic formulas for Φ in those two limits.

2. Low temperature regime

The asymptotic form of Φ when $y \rightarrow \infty$ limit is obtained by keeping only terms $n = 1$ in formula (52). This leads to

$$\begin{aligned} \Phi(\alpha, \alpha', y) &= \psi_1^2(\alpha') \left(1 + \frac{2}{y^2} \frac{A_1(\alpha, \alpha')}{\psi_1(\alpha) \psi_1(\alpha')}\right) + O(\exp[-y^2/2]) \\ &= \cos^2\left(\frac{\pi \alpha'}{2}\right) \left[1 + \frac{\pi}{4y^2} (\alpha' - 1) \tan\left(\frac{\pi}{2} \alpha'\right)\right] \\ &\quad + \cos^2\left(\frac{\pi \alpha'}{2}\right) \left[(M_{\alpha, \alpha'} - 1) \tan\left(\frac{\pi}{2} M_{\alpha, \alpha'}\right) + (1 + m_{\alpha, \alpha'}) \tan\left(\frac{\pi}{2} m_{\alpha, \alpha'}\right)\right] \frac{\pi}{4y^2} + O(\exp[-y^2/2]), \end{aligned} \quad (55)$$

where $m_{\alpha, \alpha'} = \min(\alpha, \alpha')$ and $M_{\alpha, \alpha'} = \max(\alpha, \alpha')$. Notice that the term is normalized to unity (in other words, the leading term satisfies the normalization condition of Φ). Fig. 5 shows the comparison between asymptotic expression (55) and the exact formula (52) evaluated numerically. Asymptotic formula is really accurate for any α , even for y close to unity.

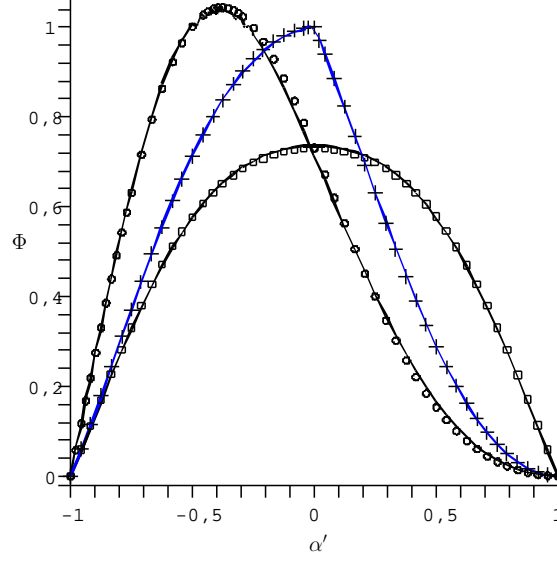


FIG. 5: Dimensionless function $\Phi(\alpha, \alpha', 2)$ for $\alpha = -0.99$ (circles), $\alpha = 0$ (plus signs) and $\alpha = 0.99$ (squares). Solid lines follow from the numerical calculation of expression (52), while points correspond to asymptotic formula (55).

3. High temperature regime

In order to obtain the small- y behaviour of Φ , the Poisson transform (90) is applied to (52). We find

$$\begin{aligned} \Phi(\alpha, \alpha', y) = & \frac{1}{2} + \frac{1}{2} \frac{(1 - \alpha) + (1 - \alpha) \sum_{n \neq 0} \exp \left[-\frac{\pi^2}{y^2} n(2n - \alpha - 1) \right]}{(1 + \alpha) + \sum_{n \neq 0} (1 + \alpha + 4n) \exp \left[-\frac{\pi^2}{y^2} n(1 + \alpha + 2n) \right]} \\ & + \frac{\sum_{n \neq 0} n \exp \left[-\frac{\pi^2}{2y^2} (\alpha' + \alpha - 2n)(\alpha' - 1 - 2n) \right] - \sum_{n \neq 0} n \exp \left[-\frac{\pi^2}{2y^2} (\alpha' - \alpha - 2n)(1 + \alpha' - 2n) \right]}{(1 + \alpha) + \sum_{n \neq 0} (1 + \alpha + 4n) \exp \left[-\frac{\pi^2}{y^2} n(1 + \alpha + 2n) \right]} \end{aligned} \quad (56)$$

for $\alpha' < \alpha$, while

$$\begin{aligned} \Phi(\alpha, \alpha', y) = & \frac{1}{2} - \frac{1}{2} \frac{(1 + \alpha) - 2 \exp \left[-\frac{\pi^2}{2y^2} (\alpha' - \alpha)(1 + \alpha') \right] + (1 + \alpha) \sum_{n \neq 0} \exp \left[-\frac{\pi^2}{y^2} n(2n - \alpha - 1) \right]}{(1 + \alpha) + \sum_{n \neq 0} (1 + \alpha + 4n) \exp \left[-\frac{\pi^2}{y^2} n(1 + \alpha + 2n) \right]} \\ & + \frac{\sum_{n \neq 0} n \exp \left[-\frac{\pi^2}{2y^2} (\alpha' + \alpha - 2n)(\alpha' - 1 - 2n) \right] + \sum_{n \neq 0} (1 - n) \exp \left[-\frac{\pi^2}{2y^2} (\alpha' - \alpha - 2n)(1 + \alpha' - 2n) \right]}{(1 + \alpha) + \sum_{n \neq 0} (1 + \alpha + 4n) \exp \left[-\frac{\pi^2}{y^2} n(1 + \alpha + 2n) \right]} \end{aligned} \quad (57)$$

for $\alpha' > \alpha$. For y small, numerical estimates of those expressions are obtained by truncating all sums to terms $n = \pm 1$. They are compared with exact formulas (56)-(57) in Fig. 6 and are quite accurate for any α , and even for y close to unity. Let us notice that, in the very high temperature regime and for almost all values of α , Φ is close to $\Theta(\alpha - \alpha')/(1 + \alpha)$.

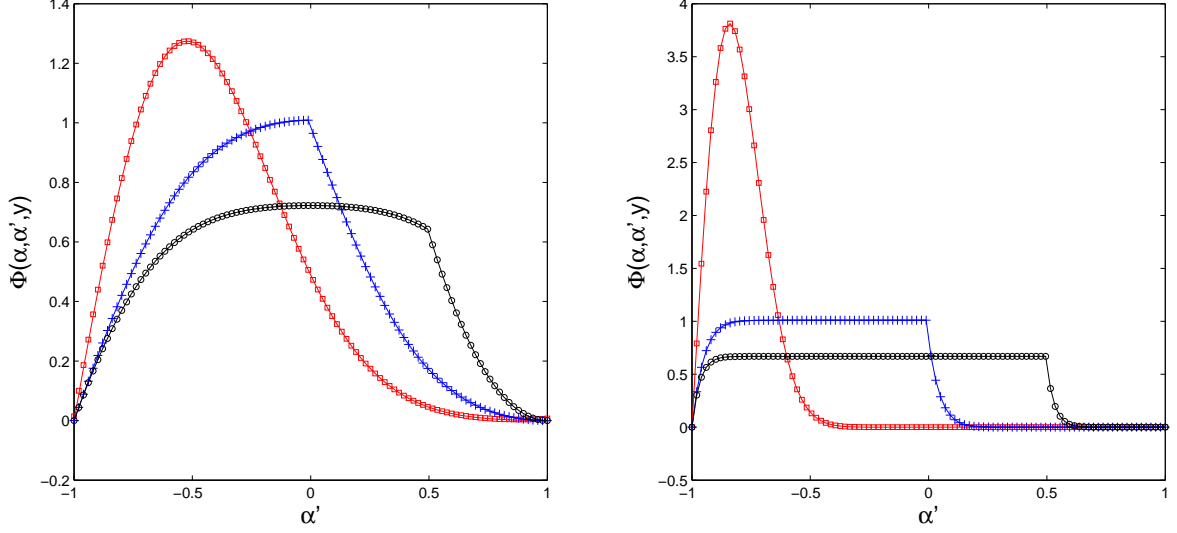


FIG. 6: Dimensionless function $\Phi(\alpha, \alpha', 1.5)$ (left panel) and $\Phi(\alpha, \alpha', 0.5)$ (right panel) for $\alpha = -0.99$ (square), $\alpha = 0$ (cross) and $\alpha = 0.5$ (circle). The solid lines follow from numerical calculations of formulas (56)-(57), while symbols correspond to small- y asymptotic formula.

V. APPLICATIONS OF THE ERGODIC APPROXIMATION FOR CONFINING POTENTIALS

In the remainder of the paper, we will restrict ourselves to a symmetric confining potential. Let us focus at first on the following question: does the ergodic approximation lead to reliable estimates in the low temperature regime? Fully analytical results will be presented for the simplest potentials, namely the harmonic potential and the infinite square well. For more complicated potentials, we combine both analytical and numerical methods.

A. Low temperature regime

1. General asymptotic formula

Inserting the asymptotic expressions (55) and (89) for Φ and g (respectively) into formula (48), we find the low-temperature behaviour of the ergodic density matrix,

$$\rho_{erg}(x, x, \beta) \stackrel{\beta \rightarrow \infty}{\sim} \int_{|x|}^{+\infty} d\ell \frac{\pi^2 \lambda_D^2}{8\ell^4} \sin^2 \left[\frac{\pi(x+\ell)}{2\ell} \right] \exp[-\beta E(\ell)] \left(\exp[-\varphi^+(\ell, x/\ell)] + \exp[-\varphi^-(\ell, -x/\ell)] \right), \quad (58)$$

with

$$\begin{aligned} E(\ell) &= \frac{\pi^2 \hbar^2}{8m\ell^2} + \int_{-1}^{+1} d\alpha' \cos^2 \left(\frac{\pi\alpha'}{2} \right) V(\alpha'\ell), \\ \varphi^\pm(\ell, \alpha) &= \frac{2m\ell^2}{\pi\hbar^2} \int_{-1}^{+1} d\alpha' (\alpha' - 1) \tan \left(\frac{\pi\alpha'}{2} \right) \cos^2 \left(\frac{\pi\alpha'}{2} \right) V(\pm\alpha'\ell) \\ &\quad + \frac{2m\ell^2}{\pi\hbar^2} \int_{-1}^{+1} d\alpha' V(\pm\alpha'\ell) \cos^2 \left(\frac{\pi\alpha'}{2} \right) \left[(M_{\alpha, \alpha'} - 1) \tan \left(\frac{\pi}{2} M_{\alpha, \alpha'} \right) + (1 + m_{\alpha, \alpha'}) \tan \left(\frac{\pi}{2} m_{\alpha, \alpha'} \right) \right] \\ &= \frac{2m\ell^2}{\pi\hbar^2} \left[2 \int_0^1 d\alpha' V(\alpha'\ell) \sin(\pi\alpha') \alpha' - \int_\alpha^1 d\alpha' V(\alpha'\ell) \sin(\pi\alpha') \right] \\ &\quad + \frac{2m\ell^2}{\pi\hbar^2} \alpha \tan \left(\frac{\pi\alpha}{2} \right) \left[\int_0^1 d\alpha' V(\alpha'\ell) \cos^2 \left(\frac{\pi\alpha'}{2} \right) - \frac{1}{\alpha} \int_0^\alpha dz V(\alpha'\ell) \cos^2 \left(\frac{\pi\alpha'}{2} \right) \right]. \end{aligned} \quad (60)$$

Positivity of φ^\pm enforces the convergence of the integral in the r.h.s. of (58) (contributions from boxes with large sizes ℓ do vanish in an integrable way). Expression (58) can still be simplified in the low temperature regime ($\beta \rightarrow \infty$), by using the saddle point method. The divergence of potential $V(z)$ for z large ensures the existence of a value ℓ_0 which minimizes the function $E(\ell)$. We emphasize that ℓ_0 depends, of course, on the potential, and is attained in integral (58) only for values of x such that $|x| < \ell_0$. Assuming that the second derivative of E is well defined at ℓ_0 , we can apply the saddle point method for $|x| < \ell_0$. This provides the general result

$$\rho_{erg}(x, x, \beta) \stackrel{\beta \rightarrow \infty}{\sim} n(x) \Gamma(\beta) \quad (61)$$

for $|x| < \ell_0$. In (61), $n(x)$ is the (unnormalized) density

$$n(x) = \frac{1}{\ell_0} \sin^2 \left[\frac{\pi(x + \ell_0)}{2\ell_0} \right] \left(\exp[-\varphi^+(\ell_0, x/\ell_0)] + \exp[-\varphi^-(\ell_0, -x/\ell_0)] \right), \quad (62)$$

while the temperature dependence is entirely embedded into

$$\Gamma(\beta) = \frac{\pi^2 \lambda_D}{8\ell_0} \sqrt{\frac{2\pi\hbar^2}{m\ell_0^4 E''(\ell_0)}} \exp[-\beta E(\ell_0)]. \quad (63)$$

We stress that temperature and position dependences are factorized in formula (61), like in the exact low-temperature behaviour (17). Although the temperature dependence of the ergodic density matrix is not entirely correct (because of the presence of factor λ_D in $\Gamma(\beta)$), the quantity $E(\ell_0)$ can be identified as the ergodic groundstate energy: indeed, it controls the exponential decay of $\rho_{erg}(x, x, \beta)$ when $\beta \rightarrow \infty$. Below, we show, through several examples, that $E(\ell_0)$ is a good approximation for the real groundstate energy.

For $|x| > \ell_0$, the saddle point ℓ_0 is outside the integration range of (58). In that case, $\rho_{erg}(x, x, \beta)$ could be evaluated by expanding the involved integrand for ℓ close to $|x|$. Of course, for a given β , if x becomes sufficiently large, $\rho_{erg}(x, x, \beta)$ tends to the classical Boltzmann factor (which, by the way, vanishes exponentially fast).

2. Infinite square potential

First, let us consider the infinite square well potential

$$V(z) = \begin{cases} -V_0 & \text{if } z < |\ell_p| \\ +\infty & \text{if } z > |\ell_p| \end{cases} \quad (64)$$

which is the simplest symmetric and confining potential. Identity

$$\int_{-1}^{+1} d\alpha' \cos^2 \left(\frac{\pi\alpha'}{2} \right) \left[(M_{\alpha, \alpha'} - 1) \tan \left(\frac{\pi}{2} M_{\alpha, \alpha'} \right) + (1 + m_{\alpha, \alpha'}) \tan \left(\frac{\pi}{2} m_{\alpha, \alpha'} \right) + (\alpha' - 1) \tan \left(\frac{\pi}{2} \alpha' \right) \right] = 0 \quad (65)$$

allows us to recast expression (58) as

$$\rho_{erg}(x, x, \beta) \stackrel{\beta \rightarrow \infty}{\sim} \theta(\ell_p - |x|) \frac{1}{\ell_p} \sin^2 \left[\frac{\pi(x + \ell_p)}{2\ell_p} \right] \exp[\beta V_0] \exp \left[-\beta \frac{\pi^2 \hbar^2}{8m\ell_p^2} \right]. \quad (66)$$

Therefore, the ergodic approximation gives the exact groundstate properties of an infinite square well. That exact results cannot be retrieved within usual approximations, like the semi-classical one.

3. Harmonic potential

For the harmonic potential $V(z) = m\omega^2 z^2/2$, we find

$$E(\ell) = \frac{\pi^2 \hbar^2}{8m\ell^2} + m\omega^2 \ell^2 \frac{(\pi^2 - 6)}{6\pi^2}. \quad (67)$$

The minimum of that expression is reached for

$$\ell_0 = \left(\frac{\pi^2 \hbar}{2m\omega} \sqrt{\frac{3}{\pi^2 - 6}} \right)^{1/2}, \quad (68)$$

and it reduces to

$$E(\ell_0) = \frac{\hbar\omega}{2} \left[\frac{\pi^2 - 6}{3} \right]^{1/2} \approx 1.14 \frac{\hbar\omega}{2}. \quad (69)$$

Since the second derivative $E''(\ell_0) = 4m\omega^2(\pi^2 - 6)/(3\pi^2)$ is well defined, it is possible to apply formula (61) for $|x| < \ell_0$. Using

$$\varphi^\pm(\ell_0, \pm x/\ell_0) = \frac{1}{4(\pi^2 - 6)} \left[-24 + \pi^2 \left(1 - \frac{x^2}{\ell_0^2} \right) \left(3 + \pi \frac{x}{\ell_0} \tan \left(\frac{\pi x}{2\ell_0} \right) \right) \right], \quad (70)$$

we eventually obtain for $|x| < \ell_0$,

$$n(x) = \frac{2}{\ell_0} \sin^2 \left[\frac{\pi(x + \ell_0)}{2\ell_0} \right] \exp \left[\frac{1}{4(\pi^2 - 6)} \left[24 + \pi^2 \left(\frac{x^2}{\ell_0^2} - 1 \right) \left(3 + \pi \frac{x}{\ell_0} \tan \left(\frac{\pi x}{2\ell_0} \right) \right) \right] \right] \quad (71)$$

$$\Gamma(\beta) = \frac{\sqrt{2\pi}\lambda_D}{8\ell_0} \exp[-\beta E(\ell_0)]. \quad (72)$$

The normalized groundstate probability density, $\Psi(x) = n(x)/\int dz n(z)$ is compared in Fig. 7 with the exact Gaussian groundstate wavefunction.

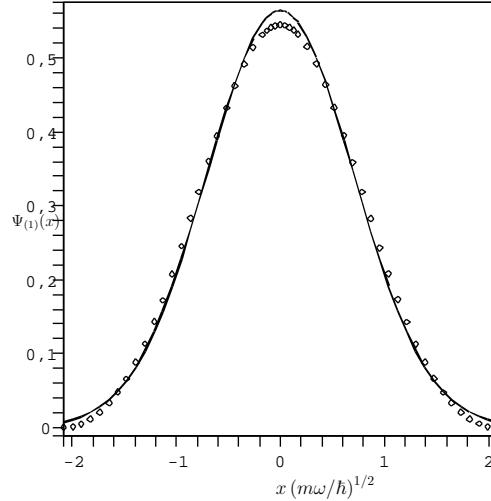


FIG. 7: Probability density of the ground state for the harmonic oscillator. The solid line represents the exact solution while points correspond to the ergodic approximation (71).

4. Anharmonic potentials

Now, we consider more complicated potentials $V(z) = a_n z^n/n$, where n is an even integer. The associated Schrödinger equation depends only on the two parameters \hbar^2/m and a_n . Only one typical energy $\varepsilon_p = (\hbar^2/m)^{n/(n+2)} a_n^{2/(n+2)}$ and one typical length $\ell_p = [\hbar^2/(ma_n)]^{1/(n+2)}$ can be built in terms of those parameters. Therefore, the energy and the spatial extension of the ground state are proportional to those typical energy and length respectively. Again,

n	2	4	6	8	10
$\frac{E(\ell_0) - E_0}{E_0}$	13%	12%	10%	7.5%	6%

TABLE I: Comparison of the ergodic groundstate energy $E(\ell_0)$ derived by using formula (74), to the exact result E_0 (obtained by numerically solving Schrödinger equation). Integer n is the exponent of the anharmonic potential

formula (61) can be used to compute the ergodic density matrix elements in the low temperature regime and for $|x| < \ell_0$. First, the function $E(\ell)$ reads

$$E(\ell) = \frac{\pi^2 \hbar^2}{8m\ell^2} + \frac{a_n \ell^n}{n} R(n), \quad (73)$$

where $R(n) = \int_{-1}^1 dz \cos^2(\pi z/2) z^n$ depends on n . The minimum of above expression, reached for $\ell_0 = \ell_p (\pi^2/4R(n))^{1/(n+2)}$, is

$$E(\ell_0) = a_n \ell_0^n R(n) \left[\frac{1}{2} + \frac{1}{n} \right]. \quad (74)$$

We also find

$$\begin{aligned} \varphi^\pm(\ell_0, x/\ell_0) &= \frac{\pi}{2nR(n)} \left[2 \int_0^1 dz \sin(\pi z) z^{n+1} - \int_{x/\ell_0}^1 dz \sin(\pi z) z^n \right] \\ &+ \frac{\pi}{2nR(n)} \left(\frac{x}{\ell_0} \right) \tan \left(\frac{\pi x}{2\ell_0} \right) \left[\int_0^1 dz \cos^2 \left(\frac{\pi z}{2} \right) z^n - \frac{\ell_0}{x} \int_0^{x/\ell_0} dz \cos^2 \left(\frac{\pi z}{2} \right) z^n \right] \end{aligned} \quad (75)$$

which provides $n(x)$.

Two important comments are in order. The scaling properties of the groundstate energy and extension are indeed recovered within the ergodic approximation. Table I presents a comparison with the numerical resolution of Schrödinger equation. The agreement, already good for low values of the exponent n , becomes better when n increases. On the contrary, the semi-classical approximation completely fails, since it provides a vanishing ground state energy (see Appendix C). Comparisons for the groundstate pdf are presented in Fig. 8: the agreement is impressive.

B. High temperature regime

Either the Wigner-Kirkwood expansion or the semi-classical approximation become well-suited when the temperature increases. Does the ergodic approximation provides satisfactory results in the high temperature regime? More precisely, what part of the Wigner-Kirkwood expansion is accounted for within that approximation? The corresponding calculations are carried out in Appendix D. We obtain

$$\rho_{erg}(x, x, \beta) \stackrel{\beta \rightarrow 0}{\sim} \frac{e^{-\beta V(x)}}{\sqrt{2\pi\lambda_D}} \left[1 - \beta \frac{d^2 V}{dx^2} \frac{\lambda_D^2}{12} + \left(\beta \frac{dV}{dx} \right)^2 \frac{\lambda_D^2}{24} A_0 + o(\lambda_D^2) \right], \quad (76)$$

where A_0 is a numerical factor close to 0.8. Thus, the leading classical term is indeed recovered, while part of the \hbar^2 -correction is also correctly reproduced. At that order \hbar^2 , the discrepancy of (76) with exact expansion (14), arises from correlations between occupation times which are not taken into account in the ergodic approximation. Nevertheless, that approximation turns out to be also quite reasonable at high temperatures.

C. Intermediate temperature regime

In this last section, we present results obtained through the numerical implementation of formula (48) at intermediate temperatures. As shown below, the ergodic approximation is particularly efficient in that regime, or in other words,

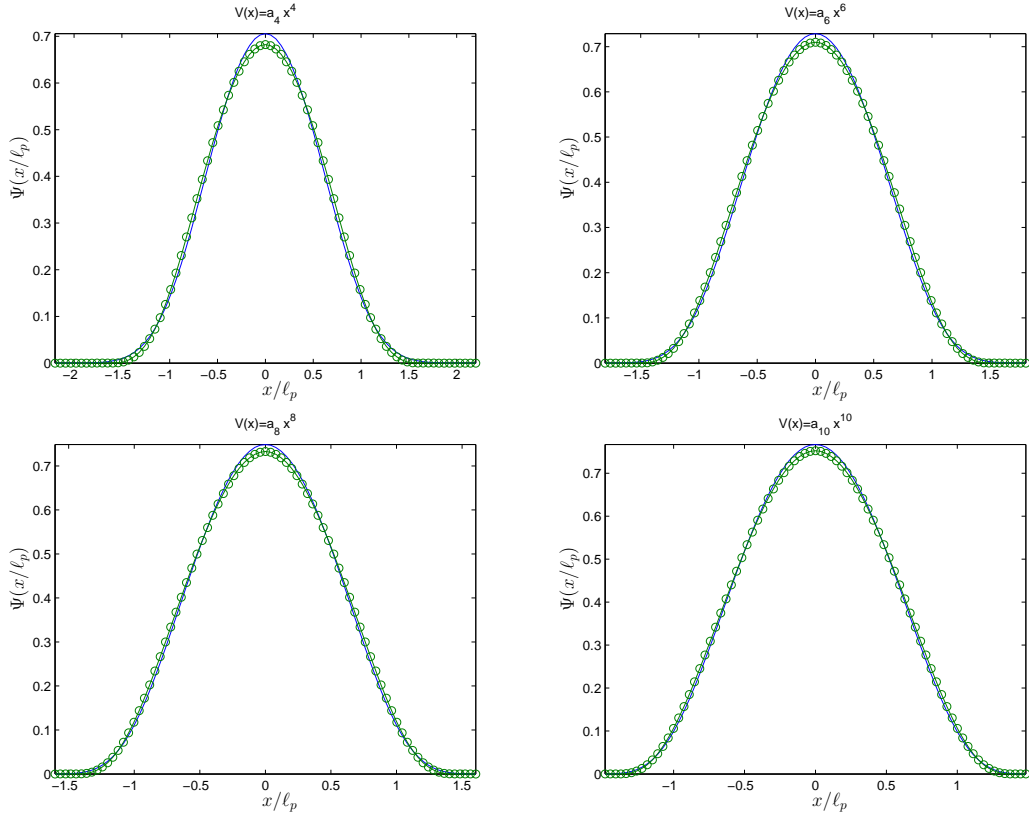


FIG. 8: Probability density function of the ground state for anharmonic oscillators. The solid line is obtained through a numerical resolution of Schrödinger equation, while points correspond to the ergodic approximation obtained from (75).

it provides a good interpolation between the exact behaviours at high and low temperatures. Here, we consider thermodynamics quantities, *i.e* the internal energy $U = -\partial_\beta (\log(Z(\beta)))$ and the probability density function (PDF) $\Psi(x, \beta) = \rho(x, x, \beta)/Z(\beta)$. Comparisons are made with either exact results or other familiar approximations.

The ergodic approximation appears to be rather accurate for estimating the considered thermodynamic quantities. For an harmonic potential, it is well-known that the semi-classical approximation turns out to be exact. As shown in figure 9, even in that case, the ergodic quantities are then close to the exact ones. For anharmonic potentials, there always exists a large-temperature domain where the ergodic approximation is significantly better than other considered approximations. Figure 10 shows results for the potential $V(x) = x^{10}$. Above temperature domain becomes larger when the anharmonicity of the potential increases.

[1] R. P. Feynman and A. R. Hibbs, *Quantum Mechanics and Path Integrals*, McGraw-Hill, New-York (1965).
[2] B. Simon, *Functional Integration and Quantum Physics* (Academic, New York, 1979); L. S. Schulman, *Techniques and Applications of Path Integrals* (Wiley, New-York, 1981); G. Roepstorff, *Path Integral Approach to Quantum Physics* (Springer, Berlin, 1994).
[3] H. Kleinert, *Path Integrals in Quantum Mechanics, Statistics, and Polymer Physics, and Financial Markets*, World Scientific (2004).
[4] E. P. Wigner, *Physical Review* **40**, 749 (1932).
[5] J. G. Kirkwood, *Physical Review* **44**, 31 (1933); *Physical Review* **45**, 116 (1934).
[6] L. Landau and E. Lifschitz, *Statistical Physics*, Pergamon Press, (1980).
[7] R. Feynman and H. Kleinert, *Physical Review A* **34**, 5080 (1986)
[8] W. Krauth, *Introduction To Monte Carlo Algorithms*, in *Advances in Computer Simulation, Lecture Notes in Physics*, edited by J. Kertesz and I. Kondor, Springer Verlag (1998).
[9] C. Predescu, D. Sabo, and J. D. Doll, *Journal of Chemical Physics* **119**, 4641 (2003).
[10] A. Bogojević, A. Balaž and A. Belič, *Physics Letters A* **345**, 258 (2005).

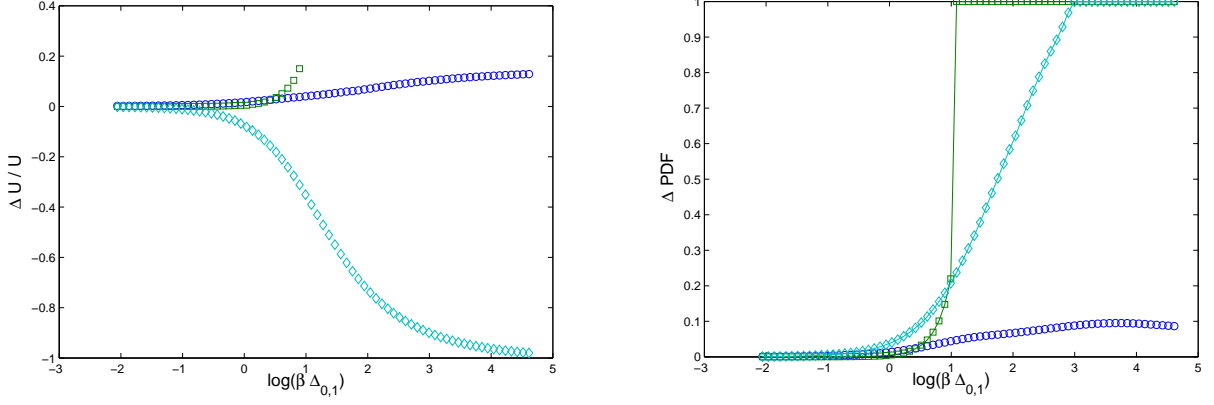


FIG. 9: Relative error for the internal energy (left panel) and mean-square error for the probability density function (right panel), as functions of the temperature for the harmonic potential. Circles correspond to the ergodic approximation, square refers to Wigner-Kirkwood expansion truncated up to order \hbar^2 and diamonds are the classical values. Quantity $\Delta_{0,1}$ is the energy gap between the ground state and the first excited one.

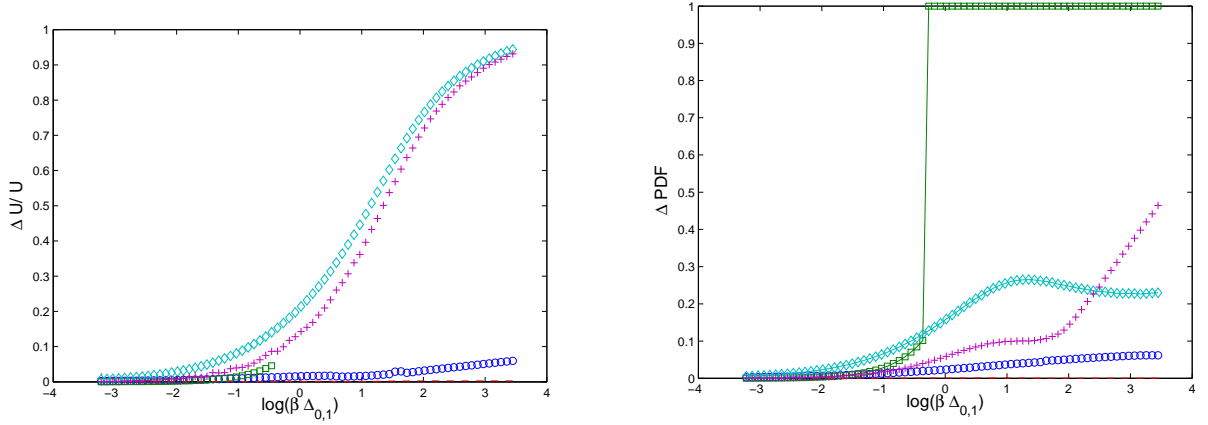


FIG. 10: Relative error for internal energy (left panel) and mean-square error for the probability density function (right panel), as functions of the temperature for the potential $V(x) = x^{10}$. The exact results are obtained by using the spectral decomposition (5). Circles correspond to the ergodic approximation, square refers to Wigner-Kirkwood expansion truncated up to order \hbar^2 , crosses describe the semi-classical approximation and diamonds are the classical values. Quantity $\Delta_{0,1}$ is the energy gap between the ground state and the first excited one.

- [11] J. P. Raffarin, general communication (2004).
 [12] J. Ginibre, *Some applications of functional integration in statistical mechanics*, in *Statistical Mechanics and Quantum Field Theory*, edited by C. DeWitt and R. Stora (Les Houches, Gordon and Breach, 1971).
 [13] F. Cornu, *Physical Review E* **53**, 4562 (1996).
 [14] D. C. Brydges and Ph. A. Martin, *Journal of Statistical Physics* **96**, 1163 (1999). Ph. A. Martin, *Actum Physica Polonica B* **34**, 3629 (2003).
 [15] T. Kihara, Y. Midzuno and T. Shizume, *J. Phys. Soc. Japan* **10**, 249 (1955).
 [16] W. Krauth, private communication (2005).
 [17] Using formula (1.441.1) and (1.441.3) from I. S. Gradshteyn, I. M. Ryzhik, *Table of Integrals Series and Products*, 5th edition, New York, Academic Press (2000), one gets

$$\sum_{n=2}^{\infty} \frac{n \sin [nx]}{n^2 - 1} = \frac{\sin(x)}{2} \left[\frac{(\pi - x)}{\tan x} - \frac{1}{2} \right], \quad \forall x \in [0, 2\pi[, \quad (77)$$

$$\sum_{n=2}^{\infty} \frac{\cos [nx]}{n^2 - 1} = \frac{1}{2} \left[1 + \frac{\cos(x)}{2} - (\pi - |x|) \sin(|x|) \right], \quad \forall x \in [-2\pi, 2\pi[. \quad (78)$$

- [18] R. Dashen, B. Hasslacher and A. Neveu, *Physical Review D* **10**, 4114 (1974).

Appendix A: Statistical weights of boxes

Eigenstates and eigenvalues of the auxiliary Hamiltonian H_ℓ^0 given in formula (18) are obtained by solving the Schrödinger equation

$$\frac{d^2\phi_\ell^0}{dz^2} = \frac{2mV_0}{\hbar^2} \left[1 - \Theta(z + \ell) + \Theta(z - \ell) - \frac{E}{V_0} \right] \phi_\ell^0(z). \quad (79)$$

The solutions are obtained by distinguishing three different regions. After introducing dimensionless function $\psi(z) = \sqrt{\ell}\phi_\ell^0(z)$ we obtain

$$\psi(x) = \begin{cases} A \exp[K(z + \ell)], & \text{if } z \leq -\ell \\ B \sin[k(z + \ell) + \delta\theta], & \forall z \in [-\ell, +\ell] \\ C \exp[-K(z - \ell)], & \text{if } z \geq \ell \end{cases}. \quad (80)$$

The continuity of the wave function and its first derivative in $\pm\ell$ leads to the following four conditions

$$A = B \sin(\delta\theta) = \frac{k}{K} B \cos(\delta\theta), \quad (81)$$

$$C = B \sin[2k\ell + \delta\theta] = -\frac{k}{K} B \cos[2k\ell + \delta\theta], \quad (82)$$

where we have introduced both wavevectors $k = (2mE)^{1/2}/\hbar$ and $K = k(V_0/E - 1)^{1/2}$. Rather than deriving the general expression for $A, C, k, \delta\theta$ as a function of B , it is sufficient to determine the asymptotic expression for large values of potential barrier V_0 . In the infinite- V_0 limit, the dominant terms are $\delta\theta \sim k/K$, $A \sim Bk/K$, $k \sim n\pi/(2\ell)$ and $C \sim (-1)^{(n-1)}Bk/K$. Finally, the value $B = 1$ is obtained through the normalization condition.

Once those results are introduced in (80), if we define the eigenvalues $E_n = \pi^2\hbar^2n^2/(8m\ell^2) = E_1n^2$ of the n -th eigenstates in the large- V_0 -limit, we then obtain the dimensionless eigenfunctions of the system in that asymptotic case

$$\psi_n(z) \stackrel{V_0 \rightarrow \infty}{\sim} \begin{cases} \sqrt{\frac{E_1}{V_0}}n, & \text{if } z = -\ell \\ \sin\left[\frac{n\pi}{2\ell}(z + \ell)\right], & \forall z \in]-\ell, +\ell[\\ (-1)^{(n-1)}\sqrt{\frac{E_1}{V_0}}n, & \text{if } z = \ell. \end{cases} \quad (83)$$

By using the spectral decomposition (5), we obtain the density matrix elements of the free particle constrained to stay in the box $[-\ell, +\ell]$

$$\rho_\ell^0(-\ell, x, \beta) = \rho_\ell^0(x, -\ell, \beta) \stackrel{V_0 \rightarrow \infty}{\sim} \frac{1}{\ell} \sqrt{\frac{E_1}{V_0}} \sum_{n=1}^{\infty} n \sin\left[\frac{n\pi}{2\ell}(z + \ell)\right] \exp[-\beta E_1 n^2], \quad (84)$$

$$\rho_\ell^0(\ell, x, \beta) = \rho_\ell^0(x, \ell, \beta) \stackrel{V_0 \rightarrow \infty}{\sim} \frac{1}{\ell} \sqrt{\frac{E_1}{V_0}} \sum_{n=1}^{\infty} (-1)^{n-1} n \sin\left[\frac{n\pi}{2\ell}(z + \ell)\right] \exp[-\beta E_1 n^2], \quad (85)$$

which leads to the following expression for the statistical weight functions

$$g^\pm(x, \ell, s, \beta) = \sqrt{2\pi} \frac{\pi^2 \lambda_D^3}{8\ell^4} S_g^\pm\left(\frac{x}{\ell}, \frac{\pi\lambda_D\sqrt{s}}{2\ell}\right) S_g^\pm\left(\frac{x}{\ell}, \frac{\pi\lambda_D\sqrt{1-s}}{2\ell}\right), \quad (86)$$

where

$$S_g^\pm(\alpha, y) = \sum_{n=1}^{\infty} n (\mp 1)^{n-1} \sin\left[n\frac{\pi}{2}(\alpha + 1)\right] \exp\left[-\frac{y^2}{2}n^2\right]. \quad (87)$$

Those two functions satisfy the equality $g^+(x, \ell, s, \beta) = g^-(-x, \ell, s, \beta)$, the normalization condition

$$\int_{|x|}^{\infty} d\ell \int_0^1 ds [g^-(x, \ell, s, \beta) + g^+(x, \ell, s, \beta)] = 1, \quad (88)$$

and they take a simple asymptotic form in the small-temperature regime

$$g \pm (x, \ell, s, \beta) \stackrel{\lambda_D \gg \ell}{\sim} \sqrt{2\pi} \frac{\pi^2 \lambda_D^3}{8\ell^4} \sin^2 \left[\frac{\pi(x + \ell)}{2\ell} \right] \exp \left[-\frac{\pi^2 \lambda_D^2}{8\ell^2} \right]. \quad (89)$$

The asymptotic expression of $g \pm$ in the high-temperature regime is obtained by taking the Poisson transform of expression (87). According to Poisson formula, if the Fourier transform of a function f exists, then, for all values of Δy

$$\Delta y \sum_{n=-\infty}^{\infty} f(n\Delta y) = \sum_{m=-\infty}^{+\infty} \int_{-\infty}^{+\infty} dz f(z) e^{-im2\pi z/\Delta y}. \quad (90)$$

Application of that transformation to expression (87) provides

$$S_g^\pm(\alpha, y) = \left(\frac{\pi}{2y^2} \right)^{3/2} \sum_{m=-\infty}^{+\infty} (1 \mp \alpha - 4m) \exp \left[-\frac{\pi^2}{8y^2} (1 \mp \alpha - 4m)^2 \right]. \quad (91)$$

Therefore, in the high temperature regime, $g \pm$ reads

$$g^-(x, \ell, s, \beta) = g^+(-x, \ell, s, \beta) \stackrel{\lambda_D \ll \ell}{\sim} \sqrt{\frac{2}{\pi}} \frac{\ell^2}{\lambda_D^3} \frac{1}{\sqrt{s(1-s)}} \frac{(1+x/\ell)^2}{s(1-s)} \exp \left[-\frac{\ell^2}{2\lambda_D^2} \frac{(1+x/\ell)^2}{s(1-s)} \right]. \quad (92)$$

Appendix B: Derivation of the mean occupation time by using the operator method

Expression (52) for the averaged occupation time $\langle \theta(x') \rangle_\omega$ can be alternatively computed by introducing the effective Hamiltonian $H_{x'} = H_\ell^0 + V_{x'}$, with $\langle x | V_{x'} = \varepsilon \delta(x - x') \langle x |$. Indeed, using a Taylor expansion of the exponential, the density matrix elements associated to that hamiltonian can be first written as

$$\frac{\langle x_i | \exp[-\beta H_{x'}] | x_f \rangle}{\langle x_i | \exp[-\beta H_\ell^0] | x_f \rangle} = \frac{\langle x_i | \exp[-\beta H_\ell^0] | x_f \rangle + \varepsilon \langle x_i | \partial_\varepsilon [\exp[-\beta H_{x'}]]_{\varepsilon=0} | x_f \rangle + O(\varepsilon^2)}{\langle x_i | \exp[-\beta H_\ell^0] | x_f \rangle} \quad (93)$$

$$= 1 + \varepsilon \frac{\langle x_i | \partial_\varepsilon [\exp[-\beta H_{x'}]]_{\varepsilon=0} | x_f \rangle}{\langle x_i | \exp[-\beta H_\ell^0] | x_f \rangle} + O(\varepsilon^2). \quad (94)$$

The Dyson derivation formula (23) and the introduction of a closure relation lead to

$$\frac{\langle x_i | \exp[-\beta H_{x'}] | x_f \rangle}{\langle x_i | \exp[-\beta H_\ell^0] | x_f \rangle} = 1 - \beta \varepsilon \frac{\int_0^1 ds \int dz \langle x_i | \exp[-\beta(1-s)H_\ell^0] | z \rangle \delta(z - x') \langle z | \exp[-\beta s H_\ell^0] | x_f \rangle}{\langle x_i | \exp[-\beta H_\ell^0] | x_f \rangle} + O(\varepsilon^2) \quad (95)$$

$$= 1 - \beta \varepsilon \frac{\int_0^1 ds \langle x_i | \exp[-\beta(1-s)H_\ell^0] | x' \rangle \langle x' | \exp[-\beta s H_\ell^0] | x_f \rangle}{\langle x_i | \exp[-\beta H_\ell^0] | x_f \rangle} + O(\varepsilon^2). \quad (96)$$

Above relation can be further simplified by introducing the wave functions $\phi_n^0(x) = \ell^{-1/2} \psi_n(x)$, given in Eq. (83), of the constrained Hamiltonian H_ℓ^0 , and its associated eigenvalues $E_n = E_1 n^2$. We obtain

$$\begin{aligned} \frac{\langle x_i | \exp[-\beta H_{x'}] | x_f \rangle}{\langle x_i | \exp[-\beta H_\ell^0] | x_f \rangle} &= 1 - \frac{\beta \varepsilon}{\ell} \frac{\int_0^1 ds \left(\sum_k \psi_k(x_i) \psi_k^*(x') e^{-\beta(1-s)E_k} \right) \left(\sum_n \psi_n(x') \psi_n^*(x_f) e^{-\beta s E_n} \right)}{\sum_n \psi_n(x_i) \psi_n^*(x_f) e^{-\beta E_n}} + O(\varepsilon^2) \quad (97) \\ &= 1 - \frac{\beta \varepsilon}{\ell} \frac{\sum_n \psi_n(x_i) |\psi_n(x')|^2 \psi_n^*(x_f) e^{-\beta E_n} + \sum_{n \neq k} \psi_k(x_i) \psi_k^*(x') \psi_n(x') \psi_n^*(x_f) \frac{e^{-\beta E_k} - e^{-\beta E_n}}{\beta(E_n - E_k)}}{\sum_n \psi_n(x_i) \psi_n^*(x_f) \exp[-\beta E_n]} + O(\varepsilon^2) \end{aligned}$$

The left-hand-side can be rewritten by using the Feynman-Kac formula as

$$\frac{\langle x_i | \exp[-\beta H_{x'}] | x_f \rangle}{\langle x_i | \exp[-\beta H_\ell^0] | x_f \rangle} = \frac{\int_{\omega} \mathcal{D}_W(\xi) \exp \left[-\beta \varepsilon \int_0^1 ds \delta(x' - x_i(1-s) - sx_f - \lambda_d \xi(s)) \right]}{\int_{\omega} \mathcal{D}_W(\xi)}. \quad (99)$$

(The effect of part H_ℓ^0 of the Hamiltonian is to restrict the integration domain to the subset ω .) Finally, using a Taylor expansion of the exponential leads to

$$\frac{\langle x_i | \exp[-\beta H_{x'}] | x_f \rangle}{\langle x_i | \exp[-\beta H_\ell^0] | x_f \rangle} = \frac{\int_{\omega} \mathcal{D}_W(\xi) \left(1 - \beta \varepsilon \int_0^1 ds \delta(x' - x_i(1-s) - sx_f - \lambda_d \xi(s)) + O(\varepsilon^2) \right)}{\int_{\omega} \mathcal{D}_W(\xi)} \quad (100)$$

$$= 1 - \beta \varepsilon \frac{\int_{\omega} \mathcal{D}_W(\xi) \int_0^1 ds \delta(x' - x_i(1-s) - sx_f - \lambda_d \xi(s))}{\int_{\omega} \mathcal{D}_W(\xi)} + O(\varepsilon^2) \quad (101)$$

$$= 1 - \beta \varepsilon \langle \theta(x') \rangle_{\omega} + O(\varepsilon^2). \quad (102)$$

Combining Eq. (98) and (102) leads to the final result (52).

Appendix C: Semi-classical approximation for potentials $V(z) = a_n z^n$ in the low-temperature regime

In this appendix, we present the semi-classical analysis for potentials $V(z) = a_n z^n$, where n is an even integer and a_n a positive real constant. The semi-classical density matrix elements are given by Dashen Formula [18]

$$\rho_{sc}(x, x, \beta) = \frac{1}{\sqrt{2\pi\hbar}} \exp \left[-\frac{S_c[\cdot]}{\hbar} \right] \left| \frac{\partial P_0(x, x_f)}{\partial x_f} \right|_{(x_f=x)}^{1/2}, \quad (103)$$

where $S_c[\cdot]$ is the classical Euclidian action of the trajectory starting from the initial point x and coming back to that point in a time $\beta\hbar$, and $P_0(x_i, x_f)$ is its initial momenta.

The classical Euclidian action for the particle moving in potential $-V$,

$$S_c[z] = \int_0^{\beta\hbar} dt \left[\frac{m}{2} \dot{z}^2 + V(z(t)) \right], \quad (104)$$

can be rewritten, if one introduces the classical energy $E = (m\dot{z}^2)/2 - V(z)$ and uses that the exponent n is even, as

$$S_c[z] = \beta\hbar E + 2 \int_0^{\beta\hbar} dt V(z(t)). \quad (105)$$

For negative energy values E , we introduce characteristic lengths $z_m = (-E/a_n)^{1/n}$ and $\ell_p = [\hbar^2/(ma_n)]^{1/(n+2)}$ and characteristic energy $\varepsilon_p = an \ell_p^n$. This leads to

$$|\dot{z}| = \left(\frac{2\varepsilon_p}{m} \right)^{1/2} \left(\frac{z_m}{\ell_p} \right)^{n/2} \left[\left(\frac{z}{z_m} \right)^n - 1 \right]^{1/2}. \quad (106)$$

Expression (105) can thus be rewritten as

$$S_c[z] = \beta\hbar\varepsilon_p \left(\frac{z_m}{\ell_p} \right)^n \left[-1 + 2 \sqrt{\frac{2}{\beta\varepsilon_p}} \left| \frac{z_m}{\lambda_D} \right| \left(\frac{\ell_p}{z_m} \right)^{n/2} \left(\frac{x}{z_m} \right)^{(n+2)/2} F_n(x/z_m) \right], \quad (107)$$

with $F_n(y) = y^{-(n+2)/2} \int_0^y du u^n / \sqrt{u^n - 1}$. The turning point z_m is determined through the constraint that the duration of the motion from z_m to x is precisely $\beta\hbar/2$.

In the more general case, if $x_i = z(0)$ is the starting point of the trajectory and $x_f = z(\beta\hbar)$ is its ending point, the constrain over time is

$$\beta\hbar = \int_{x_i}^{z_m} \left| \frac{dz}{\dot{z}} \right| + \int_{z_m}^{x_f} \left| \frac{dz}{\dot{z}} \right|. \quad (108)$$

Using expression (106), that constrain can be rewritten as

$$(2\beta\varepsilon_p)^{1/2} = \left| \frac{z_m}{\lambda_D} \right| \left(\frac{\ell_p}{z_m} \right)^{n/2} [I_n(x_i/z_m) + I_n(x_f/z_m)], \quad (109)$$

with $I_n(y) = \int_0^y du / \sqrt{u^n - 1}$. In the low temperature regime (i.e. when $\beta\hbar$ tends to infinity), we can derive the asymptotic expression of the characteristic length z_m . Setting $z_0 = z_m(x, x)$ the solution of implicit equation (109) for $x_i = x_f = x$, we calculate $z_m(x, x_f) = z_0 + \delta z$ if $x_f = x + \delta x$ is very close to x . The linearization of equation (109) then leads to

$$\frac{\delta z}{z_0} = \frac{\delta x}{x} \frac{1}{2 + (n-2) \left(\frac{z_0}{x} \right) I_n(x/z_0) [(x/z_0)^n - 1]^{1/2}}. \quad (110)$$

The quadratic case $n = 2$ is singled out since equation (109) can be analytically solve for all values of β . We obtain

$$z_0 = \frac{x}{\cosh \left[\frac{\lambda_D}{\ell_p} (\beta\varepsilon_p/2)^{1/2} \right]} \quad \text{and} \quad S_c[\cdot] = mx^2 \sqrt{\frac{2a_2}{m}} \tanh \left(\frac{\beta\hbar}{2} \sqrt{\frac{2a_2}{m}} \right) \quad (111)$$

which ultimately provides the exact density matrix. The non-quadratic cases ($n > 2$) are more interesting. At low temperatures, we find

$$z_m \sim \ell_p \left[\frac{2I_n^2 \ell_p^2}{\beta\varepsilon_p \lambda_d^2} \right]^{1/(n-2)} \quad \text{and} \quad S_c[\cdot] \sim 2|x| \sqrt{2m\varepsilon_p} \left(\frac{|x|}{\ell_p} \right)^{n/2} F_n, \quad (112)$$

where $I_n = \lim_{y \rightarrow \infty} I_n(y)$ and $F_n = \lim_{y \rightarrow \infty} F_n(y)$ are numbers of order 1, estimated numerically (see table II).

n	4	6	8	10
F_n	0.33	0.25	0.20	0.16
I_n	1.31	0.7	0.48	0.37

TABLE II: Value of F_n and I_n for different even exponents n of the potential $V(z) = a_n z^n$.

To achieve the calculation of formula (103), we have to compute the partial derivative of the initial momenta with respect to the ending point of the classical path. Energy conservation reads

$$P_0^2(x, x_f) = (2m\varepsilon_p) \left(\frac{z_m}{\ell_p} \right)^n \left[\left(\frac{x}{z_m} \right)^n - 1 \right]. \quad (113)$$

For z_m close to z_0 , we linearize $P_0(x, x_f) = P_0(x, x) + \delta P_0(x, x_f)$, with the result

$$\delta P_0(x, x_f) = \left(\frac{2m\varepsilon_n}{(x/z_0)^n - 1} \right)^{1/2} \frac{n \delta z}{2z_0}, \quad (114)$$

so

$$\left| \frac{\partial P_0(x, x_f)}{\partial x_f} \right|_{(x_f=x)} = \frac{(n/2|x|) \sqrt{2m\varepsilon_p} (z_0/\ell_p)^{n/2}}{2 [(x/z_0)^n - 1]^{1/2} + (n-2) \frac{z_0}{x} I_n(x/z_0) [(x/z_0)^n - 1]}. \quad (115)$$

In the quadratic case, we find

$$\left| \frac{\partial P_0(x, x_f)}{\partial x_f} \right|_{(x_f=x)} = \frac{\sqrt{2ma_2}}{\sinh[(\beta\hbar/m)\sqrt{2ma_2}]}.$$
 (116)

For non-quadratic cases ($n > 2$), we have the low-temperature behaviours

$$\left| \frac{\partial P_0(x, x_f)}{\partial x_f} \right|_{(x_f=x)} \sim \frac{2n}{(n-2)} \left(\frac{\ell_p}{x} \right)^n \frac{I_n \hbar \ell_p}{(2\beta\varepsilon_p)^{1/2} \lambda_D^3} \left[\frac{2I_n^2 \ell_p^2}{\beta\varepsilon_p \lambda_d^2} \right]^{(n+2)/(2n-4)}.$$
 (117)

Finally, by combining (103), (116) and (111), we obtain the exact density matrix for the harmonic potential

$$\rho_{sc}(x, x, \beta) = \frac{(2ma_2)^{1/4} \exp\left[-mx^2 \sqrt{\frac{2a_2}{m\hbar^2}} \tanh\left(\frac{\beta\hbar}{2m} \sqrt{2ma_2}\right)\right]}{(2\pi\hbar)^{1/2} \sinh[(\beta\hbar/m)\sqrt{2ma_2}]}.$$
 (118)

For anharmonic potentials, the semi-classical density matrix behaves as

$$\rho_{sc}(x, x, \beta) \sim \frac{1}{\lambda_D} \sqrt{\frac{n}{\pi(n-2)}} \left(\frac{\ell_p}{|x|} \right)^{n/2} \left(\frac{I_n \ell_p}{(2\beta\varepsilon_p)^{1/2} \lambda_D} \right)^{1/2} \left[\frac{2I_n^2 \ell_p^2}{\beta\varepsilon_p \lambda_d^2} \right]^{(n+2)/(4n-8)} \exp\left[-2|x| \sqrt{2m\varepsilon_p/\hbar^2} \left(\frac{|x|}{\ell_p} \right)^{n/2} F_n\right]$$
 (119)

When $\beta \rightarrow 0$ that expression does not reproduce the expected exponential decay with respect to temperature.

Appendix D: Ergodic density matrix at high temperatures.

Let us focus on the calculation of $\rho_{erg}(x, x, \beta)$ in the high-temperature regime. We obtain it's the asymptotical form for values of x such that $|x|/\lambda_D \gg 1$. For simplification purposes, we restrict our analysis to negative values of x . In that case, using asymptotic expression (92), we realize that we can omit the paths taken into account by the density of measure $g^+(x, \ell, s, \beta)$ since their contributions are negligible (on the contrary, for positive values of x , we can omit the contribution of paths implied in $g^-(x, \ell, s, \beta)$). Thus, expression (48) reduces to

$$\rho_{erg}(x, x, \beta) \stackrel{\beta \rightarrow 0}{\sim} \int_{-x}^{+\infty} d\ell \int_0^1 ds \frac{(\ell+x)^2}{\pi \lambda_D^4 s^{3/2} (1-s)^{3/2}} \exp\left[-\frac{(\ell+x)^2}{2\lambda_D^2 s(1-s)}\right] \times \exp\left(-\beta \int_{-1}^1 d\alpha' \left[s\Phi\left(\frac{x}{\ell}, \alpha', \frac{\pi\lambda_D\sqrt{s}}{2\ell}\right) + [1-s]\Phi\left(\frac{x}{\ell}, \alpha', \frac{\pi\lambda_D\sqrt{1-s}}{2\ell}\right) \right] V(\alpha'\ell)\right).$$
 (120)

That expression clearly shows that paths with extension larger than λ_D with respect to x give a vanishing contribution to the integrals. Since we are interested in the limit $|x|/\lambda_D \gg 1$, we see that for leading paths $x/\ell = -1 + \Delta\alpha$ with $\Delta\alpha \ll 1$. By starting from (56)-(57), we find the asymptotic form of the function $\Phi(\alpha, \alpha', y)$ in that parameter range,

$$\Phi(1 + \Delta\alpha, -1 + \Delta\alpha', y) \stackrel{\Delta\alpha \ll 1}{\sim} \begin{cases} \Phi_1(\Delta\alpha, \Delta\alpha', y) = \frac{1}{\Delta\alpha} \left[1 - \exp\left(-\frac{\pi^2}{2y^2}(\Delta\alpha' + \Delta\alpha)\Delta\alpha'\right) \right] & , \forall \Delta\alpha' < \Delta\alpha \\ \Phi_2(\Delta\alpha, \Delta\alpha', y) = \frac{2}{\Delta\alpha} \exp\left(-\frac{\pi^2}{2y^2}\Delta\alpha'^2\right) \sinh\left(\frac{\pi^2}{2y^2}\Delta\alpha\Delta\alpha'\right) & , \forall \Delta\alpha' > \Delta\alpha \end{cases}$$
 (121)

Then, the integral appearing in the exponential of (120) can be calculated by using a Taylor expansion of the potential around the position x . We obtain

$$\int_{-1}^1 d\alpha' \left[s\Phi\left(\frac{x}{\ell}, \alpha', \frac{\pi\lambda_D\sqrt{s}}{2\ell}\right) + [1-s]\Phi\left(\frac{x}{\ell}, \alpha', \frac{\pi\lambda_D\sqrt{1-s}}{2\ell}\right) \right] V(\alpha'\ell) = V(x) + \sum_{k=1}^{\infty} [V_k(\ell, s) + V_k(\ell, 1-s)]$$
 (122)

with

$$V_k(\ell, u) = u \frac{\ell^k}{k!} \frac{d^k V}{dx^k} \int_0^2 dz \Phi\left(1 + \Delta\alpha, -1 + z, \frac{\pi\lambda_D\sqrt{u}}{2\ell}\right) (z - \Delta\alpha)^k.$$
 (123)

The explicit forms of the first terms are

$$V_1(\ell, u) = -\frac{1}{2} \frac{dV}{dx} \left[u(\ell + x) - u^{3/2} \sqrt{\frac{\pi}{2}} \lambda_D \exp\left(\frac{(\ell + x)^2}{2\lambda_D^2 u}\right) \operatorname{erfc}\left(\frac{\ell + x}{\lambda_D \sqrt{2u}}\right) \right], \quad (124)$$

and

$$V_2(\ell, u) = \frac{1}{2} \frac{d^2V}{dx^2} \left[\frac{1}{3} u(\ell + x)^2 + \frac{1}{2} u^2 \lambda_D^2 - u^{3/2} \sqrt{\frac{\pi}{2}} \lambda_D (\ell + x) \exp\left(\frac{(\ell + x)^2}{2\lambda_D^2 u}\right) \operatorname{erfc}\left(\frac{\ell + x}{\lambda_D \sqrt{2u}}\right) \right],$$

where $\operatorname{erfc}(z)$ is the complementary error function. Expression (120) can be formally rewritten as

$$\rho_{erg}(x, x, \beta) \stackrel{\beta \rightarrow 0}{\sim} \int_{-x}^{+\infty} \frac{d\ell}{dx} \int_0^1 \frac{ds (\ell + x)^2}{\pi \lambda_D^4 s^{3/2} (1-s)^{3/2}} \exp\left(-\frac{(\ell + x)^2}{2\lambda_D^2 s(1-s)} - \beta V(x) - \beta \sum_{k=1}^{\infty} [V_k(\ell, s) + V_k(\ell, 1-s)]\right). \quad (125)$$

Since the temperature is high, part of the exponential implying derivatives of the potential can be expanded in power series. The truncation of these series up to second order with respect to λ_D provides

$$\begin{aligned} \rho_{erg}(x, x, \beta) = & \frac{e^{-\beta V(x)}}{\sqrt{2\pi} \lambda_D} \int_{-x}^{+\infty} \frac{d\ell}{dx} \int_0^1 ds \sqrt{\frac{2}{\pi}} \frac{(\ell + x)^2}{\lambda_D^3 s^{3/2} (1-s)^{3/2}} \exp\left(-\frac{(\ell + x)^2}{2\lambda_D^2 s(1-s)}\right) \\ & \times \left\{ 1 - \beta [V_1(\ell, s) + V_1(\ell, 1-s)] - \beta [V_2(\ell, s) + V_2(\ell, 1-s)] \right. \\ & \left. + \frac{\beta^2}{2} [V_1(\ell, s) + V_1(\ell, 1-s)]^2 + o(\lambda_D^2) \right\}. \end{aligned} \quad (126)$$

After computing the remaining integrals over s and ℓ we eventually obtain

$$\rho_{erg}(x, x, \beta) = \frac{e^{-\beta V(x)}}{\sqrt{2\pi} \lambda_D} \left[1 - \beta \frac{d^2V}{dx^2} \frac{\lambda_D^2}{12} + \left(\beta \frac{dV}{dx}\right)^2 \frac{\lambda_D^2}{24} A_0 + o(\lambda_D^2) \right], \quad (127)$$

with

$$\begin{aligned} A_0 = & -\frac{1}{2} + 3\sqrt{2\pi} \int_0^1 ds \left(\frac{s}{1-s}\right)^{3/2} \int_0^\infty dz z^2 \operatorname{erfc}^2\left(\frac{z}{\sqrt{2s}}\right) \exp\left(-\frac{z^2(2s-1)}{2s(1-s)}\right) \\ & + 3\sqrt{2\pi} \int_0^1 ds \int_0^\infty dz z^2 \operatorname{erfc}\left(\frac{z}{\sqrt{2s}}\right) \operatorname{erfc}\left(\frac{z}{\sqrt{2(1-s)}}\right), \end{aligned} \quad (128)$$

a numerical factor close 0.8 (estimated numerically to 0.796).